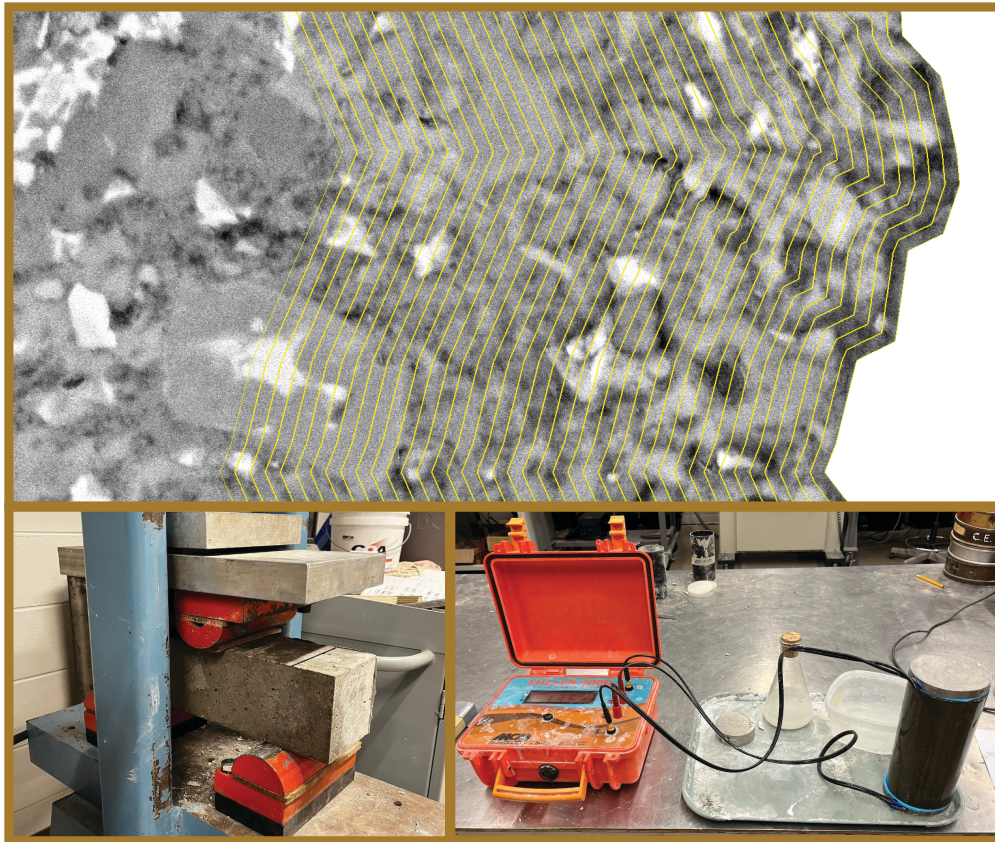


JOINT TRANSPORTATION RESEARCH PROGRAM

INDIANA DEPARTMENT OF TRANSPORTATION
AND PURDUE UNIVERSITY



Systematic Study of Type 1L Cement for Mixture Optimization and Carbon Reduction



Jookyeung Sung, Rui He, Na Lu, and Yining Feng

RECOMMENDED CITATION

Sung, J., He, R., Lu, N., & Feng, Y. (2025). *Systematic study of type 1L cement for mixture optimization and carbon reduction* (Joint Transportation Research Program Publication No. FHWA/IN/JTRP-2025/27). West Lafayette, IN: Purdue University. <https://doi.org/10.5703/1288284318575>

AUTHORS

Jookyeung Sung 

Graduate Research Assistant
Lyles School of Civil and Construction Engineering
Purdue University

Rui He 

Post-doctoral Researcher
Lyles School of Civil and Construction Engineering
Purdue University

Na (Luna) Lu, PhD 

ACPA Professor
Lyles School of Civil and Construction Engineering
Purdue University
(765) 494-5842
luna@purdue.edu
Corresponding Author

Yining Feng, PhD 

Research Assistant Professor
Lyles School of Civil and Construction Engineering
Purdue University

JOINT TRANSPORTATION RESEARCH PROGRAM

The Joint Transportation Research Program serves as a vehicle for INDOT collaboration with higher education institutions and industry in Indiana to facilitate innovation that results in continuous improvement in the planning, design, construction, operation, management and economic efficiency of the Indiana transportation infrastructure. Learn more at engineering.purdue.edu/JTRP.

Published reports of the Joint Transportation Research Program are available at docs.lib.purdue.edu/jtrp/.

NOTICE

The contents of this report reflect the views of the authors, who are responsible for the facts and the accuracy of the data presented herein. The contents do not necessarily reflect the official views and policies of the Indiana Department of Transportation or the Federal Highway Administration. The report does not constitute a standard, specification, or regulation.

TECHNICAL REPORT DOCUMENTATION PAGE

1. Report No. FHWA/IN/JTRP-2025/27	2. Government Accession No.	3. Recipient's Catalog No.	
4. Title and Subtitle Systematic study of type 1L cement for mixture optimization and carbon reduction		5. Report Date October 21, 2025	
		6. Performing Organization Code	
7. Author(s) Jookyeung Sung (https://orcid.org/0009-0004-8296-7369) Rui He (https://orcid.org/0000-0001-5039-2952) Na (Luna) Lu, PhD (https://orcid.org/0000-0002-6367-1341) Yining Feng, PhD (https://orcid.org/0000-0001-5683-0079)		8. Performing Organization Report No. FHWA/IN/JTRP-2025/27	
9. Performing Organization Name and Address Joint Transportation Research Program Hall for Discovery and Learning Research (DLR), Suite 204 207 S. Martin Jischke Drive West Lafayette, IN 47907		10. Work Unit No.	
		11. Contract or Grant No. SPR-4823	
12. Sponsoring Agency Name and Address Indiana Department of Transportation (SPR) State Office Building 100 North Senate Avenue Indianapolis, IN 46204		13. Type of Report and Period Covered Final Report	
		14. Sponsoring Agency Code	
15. Supplementary Notes Conducted in cooperation with the U.S. Department of Transportation, Federal Highway Administration.			
16. Abstract <p>The use of Portland Limestone Cement (PLC, Type 1L), a sustainable alternative to Ordinary Portland Cement (OPC), has gained traction in the United States as a means to reduce the carbon footprint associated with concrete production. Despite its environmental benefits, the inconsistent field performance, particularly with respect to strength development, durability, and admixture compatibility, has raised concerns about its application. This study aims to systematically evaluate the performance of PLCs in terms of material properties, mechanical behavior, durability, and microstructural characteristics, with the goal of informing optimized mixture designs and supporting broader implementation of PLC in infrastructure applications.</p> <p>Three cement systems—one OPC and two PLCs—were characterized using quantitative X-ray diffraction (QXRD), thermogravimetric analysis (TGA), X-ray fluorescence (XRF), and particle size distribution analysis. Nine concrete mixtures were prepared using these cements, with and without two types of water-reducing admixtures (polycarboxylate-based and lignosulfonate-based), to investigate the influence of admixtures on fresh and hardened properties.</p> <p>The results revealed variability in PLC performance, driven by differences in gypsum content, limestone content, particle size distribution, and alkali levels. PLC1, with the higher gypsum content, exhibited enhanced early-age strength and improved resistance to chloride penetration due to accelerated hydration and densified pore structure. However, its long-term compressive strength was lower than that of OPC and PLC2, attributable to its lower Belite content and higher CH (calcium hydroxide) concentration. PLC2 demonstrated higher flexural strength and a more favorable balance between early-age performance and long-term strength development.</p> <p>Durability assessments, including resistivity, void content, water absorption, and rapid chloride penetration tests (RCPT), confirmed that PLC1 achieved the most refined microstructure but did not translate into superior compressive strength due to an accumulation of weak hydration products in the interfacial transition zone (ITZ). Advanced Back Scattered Electron (BSE) – Scanning Electron Microscope (SEM) image analysis of ITZ characteristics showed that while PLC concretes generally formed thinner ITZs due to the filler effect, the addition of water reducers paradoxically increased ITZ porosity, particularly in PLC1, where high CH accumulation diminished mechanical performance.</p> <p>Overall, this study underscores the necessity of tailored mixture designs for different PLC sources to achieve optimal performance. The findings highlight that not all PLCs perform equivalently, and their compatibility with admixtures must be carefully considered. Recommendations include performance-based specifications for PLC usage and targeted SCM additions to stabilize long-term strength. This work provides a solid foundation for the implementation of PLC for constructing durable, low-carbon infrastructure and informs design practices aimed at maximizing both environmental and structural benefits.</p>			
17. Key Words type 1L cement; interfacial transition zone (ITZ); water reducer; strength; durability;		18. Distribution Statement No restrictions. This document is available through the National Technical Information Service, Springfield, VA 22161.	
19. Security Classif. (of this report) Unclassified	20. Security Classif. (of this page) Unclassified	21. No. of Pages 27	22. Price

EXECUTIVE SUMMARY

Introduction

With the increasing urgency to reduce carbon emissions in the construction sector, Portland Limestone Cement (PLC), classified as Type 1L under ASTM C595 (ASTM International [ASTM], 2024a), has emerged as a promising alternative to Ordinary Portland Cement (OPC). The primary environmental advantage of PLC lies in its ability to reduce the clinker content—thereby lowering carbon dioxide emissions—through partial substitution with finely ground limestone. As of early 2024, PLC has been accepted in all 50 U.S. states for various construction applications, reflecting growing regulatory and industry support for sustainable cementitious materials.

Despite its environmental benefits, field implementation of PLC has encountered challenges, including inconsistent mechanical performance, admixture incompatibility, and variable durability, particularly when used with traditional OPC-based mix designs. These discrepancies often stem from inherent differences in limestone content, fineness, gypsum levels, and raw material sources among commercial PLC products.

The objective of this study was to systematically investigate the performance of two commercially available PLCs compared to a reference OPC, with a focus on mechanical strength, durability, and microstructural characteristics. The influence of different water-reducing admixtures—polycarboxylate (PCE) and lignosulfonate (Lignin)—was also assessed. The findings aim to inform optimized mixture designs and provide guidelines for the broader, performance-based adoption of PLC in concrete infrastructure.

Findings

Material Characterization

The two PLCs analyzed in this study exhibited distinct chemical and physical properties. PLC1 had a higher gypsum and alkali content, while PLC2 contained finer particles and higher Belite content. These differences led to notable variations in hydration behavior, early-age strength, and long-term durability.

Fresh and Hardened Properties

All mixtures with water reducers showed improved workability. PLC1 showed higher early-age strength due to its high gypsum content, which promoted rapid hydration, but its long-term compressive strength was limited by low Belite content. PLC2 demonstrated more balanced strength development and better flexural performance. The addition of water reducers tended to delay setting and modify hydration kinetics; PCE generally had a stronger effect than Lignin.

Durability Performance

PLC1 consistently showed higher resistivity and lower chloride permeability than OPC and PLC2, indicating a denser microstructure. However, it also exhibited higher shrinkage and lower long-term strength. Void content and water absorption tests confirmed that PLC1 had a more refined pore structure, although this did not translate to higher mechanical strength due to excessive calcium hydroxide (CH) accumulation. Rapid Chloride Penetration Tests (RCPT) aligned with resistivity findings, confirming that PLC1 performed well in mitigating chloride ingress.

ITZ and Microstructural Analysis

Backscattered electron (BSE) image analysis revealed that PLC concretes generally exhibited thinner interfacial transition zones (ITZ) than OPC due to the filler effect of limestone. However, the use of water reducers increased ITZ porosity and, in the case of PLC1, led to CH accumulation around aggregates, which weakened the ITZ and suppressed strength development. The image analysis method also revealed that ITZ porosity and CH distribution play a critical role in mechanical performance.

Implementation

This study provides actionable insights for practitioners and agencies adopting PLC in structural and pavement concrete. The results emphasize that not all PLCs are created equal, and their performance highly depends on gypsum content, limestone fineness, and compatibility with chemical admixtures. As a result, direct substitution of OPC with PLC in existing mix designs may lead to less desirable performances.

For successful implementation, it is recommended that performance-based specifications be prioritized over prescriptive cement content limits. Designers should consider tailoring water reducer type and dosage according to the specific chemical and mineralogical characteristics of the PLC being used. Furthermore, PLCs with moderate gypsum and high Belite content (like PLC2) may provide a better balance between strength and durability, especially when combined with supplementary cementitious materials (SCMs).

The research also highlights the critical role of ITZ in determining long-term concrete performance. Advanced imaging techniques such as Scanning Electron Microscopy (SEM)-BSE and Energy Dispersive X-ray Spectroscopy (EDS) mapping can help inform material selection and mix optimization in high-performance concrete.

From an environmental standpoint, both PLCs offer reduced embodied carbon compared to OPC, reinforcing their potential in sustainable infrastructure. However, these gains must be balanced with performance and life-cycle cost considerations. The outcomes of this study can guide state departments of transportation, contractors, and material suppliers in refining their specifications and adopting PLC mixtures that deliver both durability and decarbonization benefits.

CONTENTS

1. INTRODUCTION	8
1.1 Research Background	8
1.2 Problem Statement	8
1.3 Research Objectives	8
1.4 Organization of the Report.	8
2. LITERATURE REVIEW	8
2.1 PLC: Characteristics and Performance Parameters	8
2.2 Field Performance Issues with Commercial PLC	9
2.3 Importance of the Interfacial Transition Zone (ITZ) in Concrete.	9
3. COMPARATIVE EVALUATION OF OPC AND PLC: MATERIAL CHARACTERISTICS, MECHANICAL AND DURABILITY PERFORMANCE	10
3.1 Raw Cement Characterization	11
3.1.1 Quantitative X-Ray Diffraction (QXRD) Result	11
3.1.2 Calcite Content Calculation through Thermogravimetric Analysis (TGA).	12
3.1.3 X-Ray Fluorescence (XRF) Result	12
3.1.4 Particle Size Distribution Result	12
3.2 Mixture Design.	13
3.3 Fresh and Harden Concrete Properties.	13
3.3.1 Slump Test Result.	13
3.3.2 Setting Time Result	13
3.3.3 Isothermal Calorimetry Test Result	13
3.3.4 TGA results	16
3.3.5 Shrinkage Test.	16
3.4 Mechanical Properties	17
3.4.1 Compressive Strength.	17
3.4.2 Flexural Strength	18
3.5 Durability Properties	18
3.5.1 Bulk and Surface Resistivity Test Result	18
3.5.2 Void Content Result.	20
3.5.3 Water Absorption Test Result.	20
3.5.4 RCPT Result	20
3.6 Summary	20
4. ITZ EVALUATION THROUGH SCANNING ELECTRON MICROSCOPE SEM-BSE IMAGE ANALYSIS	21
4.1 Image Analysis Process	22
4.1.1 Image Collection and Preprocessing	22
4.1.2 Defining Breakpoint and Strip Delineation	22
4.1.3 Porosity Result	23
4.2 CH Content.	23
4.3 Summary	23
5. FINAL CONCLUSIONS AND RECOMMENDATIONS	24
5.1 Conclusions	24
5.2 Recommendations	25
REFERENCES	25

LIST OF TABLES

Table 3.1 Mineral Contents of Raw Cements with ZnO Determined by QXRD.	11
Table 3.2 Oxide Contents of Raw Cements by XRF.	12
Table 3.3 Particle Size and Surface Area Characteristics of Cements.	13
Table 3.4 Mixture Proportions of Concrete.	13
Table 3.5 Slump Values of Different Mixtures (Data in Brackets is the Slump Increase Compared to the Plain Mixture).	14
Table 4.1 The Estimated Thickness of the ITZ.	23
Table 4.2 The Average Porosity of the ITZ.	23

LIST OF FIGURES

Figure 2.1	Schematic Image of “Wall Effect” Based on Scrivener et al. (Scrivener et al., 2004; B. Wang et al., 2021).	10
Figure 3.1	XRD Diffraction Patterns of Raw Cements.	11
Figure 3.2	Calcite (CaCO_3) Content Calculation Through TGA Result.	12
Figure 3.3	Particle Size Distribution of Cements by (a) Volume (%) and (b) Cumulative Volume (%).	13
Figure 3.4	Photos of the Slump Test.	14
Figure 3.5	The Setting Time of Different Concrete Mixtures.	14
Figure 3.6	IC Test Results of Plain Mixtures Without Water Reducers.	15
Figure 3.7	The Heat Flow of All Mixtures.	15
Figure 3.8	Total Released Heat of All Mixtures.	15
Figure 3.9	Calcium Hydroxide (CH) Content Determined by TGA Analysis.	16
Figure 3.10	Shrinkage of All Mixtures at 50% RH and 100% RH.	16
Figure 3.11	Comparison Graph of the Compressive Strength of All Mixtures With Different Water Reducers.	17
Figure 3.12	Comparison of Compressive Strength Development in Different Cement Systems.	17
Figure 3.13	Compressive Strength in Terms of CH Content.	18
Figure 3.14	Flexural Strength of All Mixtures at 28 Days of Curing.	18
Figure 3.15	Flexural-to-Compressive Strength Ratio of All Mixtures.	18
Figure 3.16	Comparison Graph of the Bulk Resistivity Results of All Mixtures.	19
Figure 3.17	Comparison Graph of the Surface Resistivity Test Results of All Mixtures.	19
Figure 3.18	Formation Factor in Terms of Compressive Strength.	20
Figure 3.19	Comparison Graph of the Void Content Results Based on the Water Reducers (28 Days).	20
Figure 3.20	Water Absorption Test Result With Initial Absorption Rate (I_{ini}) and Secondary Absorption Rate (I_{sec}).	21
Figure 3.21	RCPT Result of All Mixtures.	21
Figure 4.1	Flowchart of Analysis Method for Defining ITZ Thickness.	22
Figure 4.2	The Example Graph for the Application of PLR.	22
Figure 4.3	The Example of the BSE Image with Strip Delineation.	22
Figure 4.4	ITZ Porosity Analysis Results.	23
Figure 4.5	Element Distribution Around the Aggregate.	24
Figure 4.6	CH Content Around the Aggregate Surface.	24

1. INTRODUCTION

1.1 Research Background

The carbon dioxide gas emissions associated with the manufacture of Ordinary Portland Cement (OPC) have been highlighted recently. According to the U.S. Environmental Protection Agency (2021), approximately 3% of all emissions in the United States are generated by the OPC manufacturing process, and this is expected to increase as global demand for concrete continues to grow. To improve environmental sustainability, the concrete industry is seeking substitute materials that reduce OPC usage without compromising performance.

The Portland Limestone Cement (PLC), as defined by ASTM C595 as Type 1L cement (ASTM, 2024a), is suggested for lowering the amount of clinker. One approach is to replace the cement clinker with limestone, making it a viable substitute for OPC throughout North America, including the United States. According to a recent report, the acceptance of PLC by state Departments of Transportation (DOTs) in the United States has gradually increased over the past decade. As of February 2024, all 50 states have adopted PLC. This substitution significantly reduces the clinker content, thereby lowering energy consumption and carbon dioxide emissions during cement manufacturing (Tennis et al., 2011).

1.2 Problem Statement

The commercial PLC products on the market exhibit differences in terms of limestone content, particle size distribution, and raw material composition. These differences, often stemming from variations in mineralogy, raw material sources, and kiln operations, have led to unpredictable outcomes in concrete strength, durability, and admixture compatibility (Barrett, 2013; Tennis et al., 2011).

The conventional mix designs developed for OPC may not be suitable for PLC mix designs. Users in the field have reported lower strength and inconsistent performance with water-reducing admixtures. The changes in early hydration behavior and microstructural development, particularly at the interfacial transition zone (ITZ), may lead to poor compressive and flexural strength.

Barrett et al. (2014) used the experimental evaluation of three commercially available PLCs for a year to confirm the importance of these problems. They demonstrated that finer limestone particles, whether intergrounded or blended, influenced early-age strength development and shrinkage behavior. While properly ground PLCs performed similarly to OPC in mechanical tests, the study revealed that performance consistency is sensitive to the fineness of limestone, its content, and the water-to-powder ratio. These findings highlighted the importance of accounting for such material variability when evaluating or implementing PLC.

These issues promoted the need to systematically evaluate PLC regarding mechanical performance, durability, and compatibility with chemical admixtures. Without such an assessment, the reliable application of structural concrete remains uncertain.

1.3 Research Objectives

The objective of this project is to develop a comprehensive understanding of the performance of PLC concrete incorporating various additives, providing design and construction guidance for developing high-performance and durable PLC concrete. The research team will evaluate PLC concrete for specific applications such as pavements, structural elements, bridge decks, and link slabs. A combination of mechanical tests, image analysis, and durability assessments is used to evaluate behavior. The findings are expected to highlight both the economic and environmental advantages of PLC, supporting its broader adoption and contributing to more sustainable construction practices nationwide.

1.4 Organization of the Report

This report is structured to present a comprehensive evaluation of PLC in comparison to OPC, with a focus on mixture optimization and carbon reduction. The content is organized as follows:

- *Chapter 1: Introduction*—This chapter outlines the background and motivation for the study, including the environmental benefits of PLC and the practical challenges encountered in its field application. It defines the research problem, states the objectives, and provides an overview of the report structure.
- *Chapter 2: Literature Review*—A detailed review of existing literature is presented to contextualize the study. Topics covered include the composition and hydration mechanisms of PLC, field performance issues with commercial PLC products, and the critical role of the ITZ in concrete durability and strength.
- *Chapter 3: Comparative Evaluation of OPC and PLC*—This chapter describes the experimental methodology and presents a comprehensive analysis of raw material characteristics, fresh and hardened concrete properties, and durability performance. It includes test results on slump, setting time, hydration heat, compressive and flexural strength, shrinkage, resistivity, void content, water absorption, and rapid chloride penetration.
- *Chapter 4: ITZ Evaluation through SEM-BSE Image Analysis*—Advanced microstructural characterization of the ITZ is conducted using scanning electron microscopy with backscattered electron (BSE) imaging. The analysis quantifies ITZ thickness and porosity and explores calcium hydroxide (CH) accumulation near aggregate surfaces. The effects of water reducers on ITZ quality and their correlation with mechanical performance are also discussed.

2. LITERATURE REVIEW

2.1 PLC: Characteristics and Performance Parameters

PLC is a type of blended cement in which up to 15% of the cement is replaced with finely ground limestone, following ASTM C595 (ASTM, 2024a). Given that clinker production is the most energy- and carbon-intensive stage of the cement manufacturing process, incorporating limestone as a partial replacement facilitates significant reductions in both energy consumption and carbon emissions (Tennis et al., 2011).

In addition to its environmental advantages, numerous studies have demonstrated that the limestone particles in PLC play a crucial role in enhancing strength growth and the development of durability-related qualities. Mechanistically, the action of limestone powder can be described by four significant effects: filler effect, nucleation effect, dilution effect, and chemical effect (D. Wang et al., 2018).

The filler effect describes the role of finer limestone particles than cement particles in improving particle size distribution, filling voids, and enhancing packing density, which collectively contribute to refining the microstructure. Additionally, due to their large specific surface area, fine limestone particles provide nucleation sites for hydration products such as calcium silicate hydrate (C-S-H), thereby accelerating the degree of hydration, increasing the amount of hydration products, and enhancing the hydration heat, known as the nucleation effect. However, if the particles become excessively fine and the specific surface area becomes too high, the flowability of concrete may be reduced. Furthermore, it has been reported that calcite, due to its surface structure resembling that of the calcium oxide (CaO) layers in C-S-H, is more favorable for the precipitation and growth of early hydration products. Therefore, the chemical composition of limestone (e.g., calcite vs. aragonite) can influence its nucleation effect (D. Wang et al., 2018).

The dilution effect refers to the reduction in the total heat of hydration over time due to the partial replacement of reactive clinker with limestone in cement. When the replacement exceeds 15%, this effect becomes predominant, leading to a decline in compressive strength and an increase in porosity. Furthermore, the reduction in reactive clinker content results in lower ionic concentration in the pore solution compared to OPC. Given these adverse effects on performance at high limestone content, ASTM C595 imposes limits on the allowable limestone replacement in PLC (ASTM, 2024a; Lothenbach et al., 2008).

Vuk et al. (2001) evaluated the effects of the fineness when 5% of the cement clinker is replaced with limestone. The results demonstrated that the Blaine specific surface area increased with the addition of limestone compared to its absence, leading to an increase in water demand and a reduction in both initial and final setting times. In a separate study, Tsivilis et al. (2003) reported that PLC concrete, in which 20% of the clinker was replaced with limestone, demonstrated higher total porosity than OPC concrete with comparable compressive strength, but exhibited relatively reduced water permeability and sorptivity.

In summary, PLC is a type of blended cement in which a portion of the cement clinker is replaced with limestone, as specified in ASTM C595 (ASTM, 2024a). PLC can alleviate environmental pressures by partially replacing the clinker production stage, which is the most energy and carbon intensive. Moreover, the properties of the PLC concrete rely on the physical and chemical properties of the limestone particles in cement. Numerous studies have demonstrated that limestone particles make a positive contribution to strength development and durability. However, when the replacement ratio exceeds 15%, the negative dilution effect becomes more pronounced, leading to reduced compressive strength and increased porosity.

2.2 Field Performance Issues with Commercial PLC

Despite its environmental and technical advantages, the field performance of commercial PLCs exhibits notable variability. Several studies and field observations have highlighted inconsistencies in strength development, durability, and admixture compatibility among PLCs produced by different manufacturers. These discrepancies are often attributed to variations in limestone content, fineness, and the mineralogical composition of clinker, as well as differences in grinding practices across production facilities (Barrett, 2013).

The heterogeneity of limestone sources could be the primary reason for this issue. As previously discussed, even when the limestone content remains within the allowable range (e.g., 10–15%), its physical and chemical properties, such as particle size distribution, specific surface area, and mineral phase composition, may differ significantly. These variations affect hydration kinetics, and the evolution of the cement paste microstructure, making it more challenging to predict setting behavior and strength in field applications (Barrett et al., 2014; Vuk et al., 2001; D. Wang et al., 2018).

Several field applications and lab experiments have demonstrated that the early-age strength of PLC concrete can either match or exceed that of OPC, depending on factors such as mix design, curing conditions, and the use of chemical admixtures (Barrett et al., 2014; Tennis et al., 2011). Inconsistencies in sulfate availability resulting from altered clinker-to-limestone ratios may disrupt the formation of ettringite and monosulfate phases, thereby affecting setting times and strength gain (Tennis et al., 2011). To mitigate these risks, some agencies have suggested using performance-based requirements and have suggested tighter limits on the properties of limestone. These include verifying concrete strength, shrinkage, and durability performance under relevant exposure conditions, rather than solely relying on cement composition. Moreover, the addition of supplementary cementitious materials (SCMs) has been shown to stabilize PLC performance across a broader range of field conditions (D. Wang et al., 2018).

In summary, the performance variability of commercial PLCs stems from multiple factors, making it unrealistic for each manufacturer to individually control limestone quality and operate under a unified production process. Therefore, a more realistic strategy is to understand the unique properties of each cement manufacturer and select appropriate chemical admixtures and SCMs based on those properties; this area requires further investigation. To ensure the utility and reliability of PLCs in the field, it is essential to verify consistent performance not only under controlled laboratory conditions but also in environments that replicate or reflect actual job site conditions.

2.3 Importance of the Interfacial Transition Zone (ITZ) in Concrete

The ITZ refers to the region of cement paste surrounding aggregate particles, characterized by distinct microstructural and compositional features. Although it typically spans only 10–50 μm from the aggregate surface, its influence on the

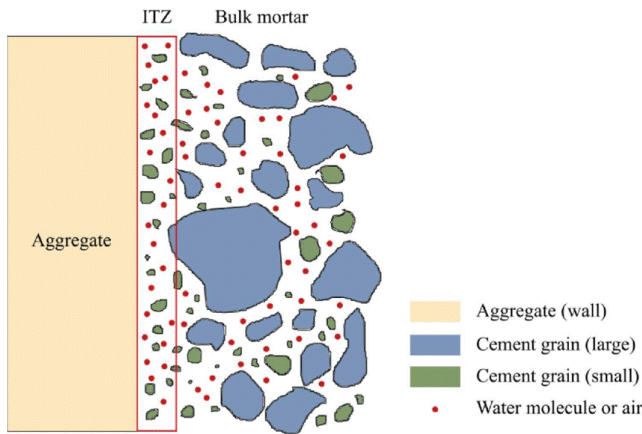


Figure 2.1 Schematic Image of “Wall Effect” Based on Scrivener et al. (Scrivener et al., 2004; B. Wang et al., 2021).

mechanical strength, durability, and transport properties of concrete is disproportionately large relative to its volume. As concrete is increasingly expected to perform under aggressive environmental conditions, the role of ITZ has garnered attention due to its susceptibility to microcracking, increased porosity, and ion transport (Ollivier et al., 1995).

The fundamental origin of the ITZ lies in a phenomenon known as the wall effect. This effect arises because aggregate particles are significantly larger than cement particles which leads to a structural constraint when cement particles encounter the relatively flat surface of the aggregate. Considering the anhydrous distribution, inserting a large object into a randomly packed assembly disrupts the arrangement of small particles. Consequently, the area next to the aggregate surface has a larger initial porosity and fewer big cement particles. The development of hydration products during the hydration process is directly influenced by the localized increase in the effective water-to-cement ratio resulting from this cement particle deficit. Hydration products, such as CH and ettringite, tend to form as larger crystals in this region compared to the bulk cement matrix, with CH tending to concentrate deposition. Consequently, a more porous microstructure develops, and even as hydration progresses and some pores are filled, the ITZ retains significantly higher porosity than the surrounding bulk paste. The ITZ is not a sharply defined boundary but rather a gradual transition zone in which microstructural characteristics change progressively between the aggregate and the cement paste. Due to its high initial porosity, concentration of specific hydration products (especially CH), and relative lack of cement particles, the ITZ is commonly regarded as the weakest link in cement-based composites. It plays a critical role in the initiation of microcracks and significantly affects transport properties, including moisture and ion permeability. (Scrivener et al., 2004; Wu et al., 2016).

Studies using BSE, energy dispersive x-ray spectroscopy (EDS), and mercury intrusion porosimetry (MIP) have consistently shown that the ITZ has coarser pores and greater total porosity compared to the bulk paste. Wu et al. (2016) reported chloride diffusion coefficients in the ITZ up to 12 times higher

than those in the surrounding bulk paste. Additionally, Gao, De Schutter, Ye, Huang, et al. (2013) demonstrated that ITZ significantly governs capillary absorption behavior, especially in concrete with high aggregate content, emphasizing its role as a primary pathway for deleterious agents such as chloride ions, sulfate ions, and carbon dioxide. Mechanically, the disparity in stiffness and strength between the ITZ and bulk paste results in stress concentration under load, which promotes the initiation and propagation of microcracks. Y. Wang et al. (2024) found that larger aggregate sizes are associated with thicker and more porous ITZs, correlating with reductions in both elastic modulus and compressive strength.

Despite its critical role, the ITZ remains among the least understood aspects of concrete microstructure. Unlike bulk paste hydration, which has been extensively characterized, studies focusing specifically on the ITZ are relatively limited due to challenges in sample preparation, imaging, and the inherent heterogeneity of the zone. Most existing knowledge stems from a small number of detailed Scanning Electron Microscopy (SEM)-BSE image analyses, which are both time-consuming and require sophisticated instrumentation (Scrivener et al., 2004). Furthermore, studies on the ITZ properties of PLC and the cement blended with limestone filler (LF) remain limited. As previously discussed, limestone enhances the density of the microstructure through the filler effect and promotes the formation of hydration products through the nucleation effect. These effects may make ITZ more dense and thinner, resulting in improved mechanical performance. Wu et al. (2016) highlighted that the addition of 5% LF was found to reduce porosity in the region near the aggregate surface (0–20 μm) and decrease the volume of larger pores (> 100 nm) typically associated with the ITZ. These findings suggest that LF may have a beneficial effect on ITZ development. However, the authors noted that the observed improvements in chloride diffusion resistance and water absorption were primarily attributed to the densification of the bulk cement matrix, with only partial contributions from changes in the ITZ. Nevertheless, the importance of further research in this area is highlighted, despite this study providing valuable quantitative insights into the ITZ microstructure of LF-blended cement.

In conclusion, the ITZ is a pivotal microstructural feature critically influencing the mechanical performance and durability of concrete. However, current research, especially regarding PLC systems, is inadequate to establish comprehensive design and performance guidelines. Addressing this gap will require focused experimental investigations employing advanced imaging and analytical techniques to achieve higher resolution and reproducibility.

3. COMPARATIVE EVALUATION OF OPC AND PLC: MATERIAL CHARACTERISTICS, MECHANICAL AND DURABILITY PERFORMANCE

This chapter presents comparative analysis results of commercially available OPC and two PLCs in diverse aspects. To evaluate the compatibility between PLC and water reducers, two different chemical bases (Polycarboxylate [PCE] and Lignosulfonate [Lignin]) of water reducers have been selected.

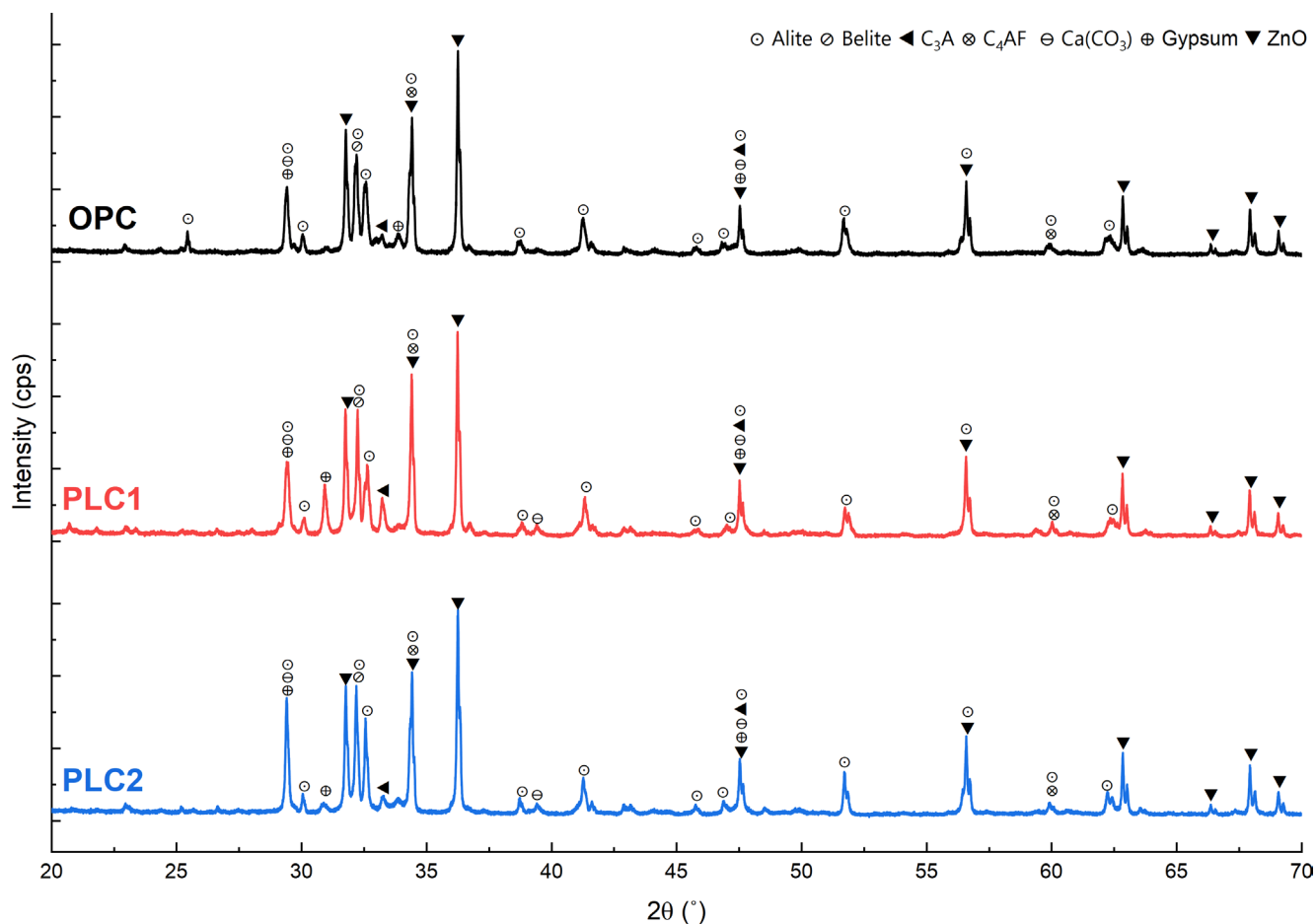


Figure 3.1 XRD Diffraction Patterns of Raw Cements.

3.1 Raw Cement Characterization

In this work, the OPC is provided by the Indiana Department of Transportation (INDOT) and two different PLCs from different manufacturers. As the physical and chemical properties of these materials are unknown, characterizing the raw cement was inevitable before mixing.

3.1.1 Quantitative X-Ray Diffraction (QXRD) Result

QXRD analysis was performed to quantify the minerals (e.g., alite, belite, tricalcium aluminate (C_3A), calcite [Limestone], and gypsum) in the raw cements, facilitating an easy comparison of their chemical compositions. Zinc oxide (ZnO), which exhibits distinct peaks from the main minerals of the cement, was added at a 20% weight ratio of the cement and uniformly blended to prepare the XRD sample.

Tricalcium silicate (alite) and dicalcium silicate (belite) form hydration products, including calcium silicate hydrate (C-S-H) and calcium hydroxide (CH), through hydration reactions. It is well known that alite primarily contributes to early strength development, while belite plays a role in long-term strength development (Odler, 1998). Through Table 3.1, the mechanical

TABLE 3.1
Mineral Contents of Raw Cements with ZnO Determined by QXRD.

Mineral (Formula)	OPC	PLC1	PLC2
Alite (C_3S)	63.26%	46.60%	47.07%
Belite (C_2S)	12.71%	22.54%	17.34%
C_4AF	10.18%	7.19%	5.91%
C_3A	7.47%	5.48%	3.37%
Calcite (Limestone)	1.15%	9.17%	3.34%
K_2SO_4	1.96%	3.33%	1.39%
Na_2SO_4	2.18%	3.48%	3.39%
Gypsum	0.64%	0.49%	8.01%
MgO	0.45%	1.63%	1.30%
CaO (Free Lime)	-	0.09%	0.22%

properties can be predicted since OPC has the highest alite, and PLC2 has the highest belite. Additionally, PLC1 and PLC2 exhibited similar calcite contents of approximately 7%.

A notable point is that PLC2 has the highest gypsum content among the others. Gypsum is added to prevent flash set, which occurs when C_3A reacts rapidly with water. It reacts with C_3A to form a layer of ettringite (Aft) around the C_3A particles, thereby interrupting further reactions and slowing down the setting time

of the cement. Moreover, it enhances early-age strength performance by promoting the dissolution of alite and accelerating hydration, thereby generating hydration products such as C-S-H and CH. Additionally, this leads to a more dispersed and controlled aluminate reaction, as demonstrated by a lower and more widespread initial peak (Quennoz & Scrivener, 2012).

3.1.2 Calcite Content Calculation through Thermogravimetric Analysis (TGA)

However, as shown in Figure 3.1, the main peak of calcite at 29.4° overlaps with alite and gypsum, which can lead to quantification errors. To address this limitation, thermogravimetric analysis (TGA) was used to determine the calcite content. In cementitious systems, limestone (calcite, CaCO_3) typically decomposes above 600 °C, producing carbon dioxide and calcium oxide, accompanied by a weight loss ($\text{WL}_{\text{CaCO}_3}$). The theoretical weight loss from calcite decomposition is approximately 44%. Based on the experimentally measured weight loss, the calcite content can be calculated using Equation 3.1. According to Figure 3.2, PLC1 and PLC2 have similar limestone content, around 10%.

$$\text{CaCO}_{3,\text{measured}} (\%) = \text{WL}_{\text{CaCO}_3} (\%) \times \frac{100}{44}$$

Equation 3.1

3.1.3 X-Ray Fluorescence (XRF) Result

The XRF analysis results revealed differences among the three cements. Consistent with the QXRD results, PLC1 contained relatively more alkali sulfates compared to the other cements, as indicated by its sulfur trioxide (SO_3) content and high equivalent alkalis. In addition, based on the equivalent alkali levels, it can be inferred that OPC and PLC2 were designed as low alkali cements (< 0.6%; ASTM C150/150M-24; ASTM, 2024b)

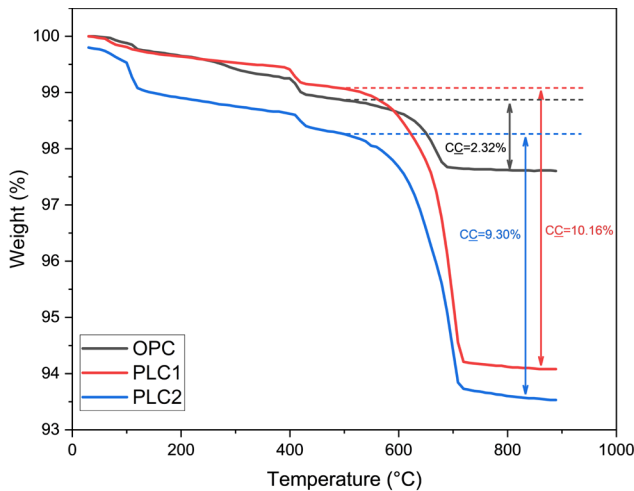


Figure 3.2 Calcite (CaCO_3) Content Calculation Through TGA Result.

TABLE 3.2
Oxide Contents of Raw Cements by XRF.

Oxides	OPC	PLC1	PLC2
CaO	68.2%	67.79%	68.48%
SiO ₂	18.21%	16.52%	17.41%
SO ₃	3.69%	4.33%	3.85%
Al ₂ O ₃	4.38%	4.03%	4.39%
MgO	1.13%	3.23%	3.53%
Fe ₂ O ₃	3.59%	2.94%	1.94%
Na ₂ O	54.9ppm	0.14%	735.8ppm
K ₂ O	0.76%	0.78%	0.23%
Equivalent alkalis	0.51%	0.65%	0.22%

3.1.4 Particle Size Distribution Result

The particle size distribution results from particle size analysis (PSA) tests are presented in Figure 3.3. Figure 3.3a shows that PLCs contain more fine particles (1~5 μm) as well as a higher proportion of coarse particles (> 20 μm) compared to OPC. The peak of PLC1 is shifted to the right relative to the other cements, indicating that it contains a higher proportion of coarse particles. However, as shown in Figure 3.3b, the overall particle size distribution ranges are quite similar among all three types of cements.

Additional calculations based on the data from the PSA test were performed to find the difference between OPC and PLCs. Span means the measurement of the width of the distribution. The narrower the distribution, the smaller the span becomes. Uniformity refers to a measure of absolute deviation from the median, and the specific surface area (SSA) is calculated as the total area of the particles divided by their total weight.

$$\text{Span} = \frac{D_{90} - D_{10}}{D_{50}}$$

Equation 3.2

$$\text{Uniformity} = \frac{\sum V_i |D_{50} - D_i|}{D_{50} \sum V_i}$$

Equation 3.3

$$\text{SSA} = \frac{6 \sum \frac{V_i}{D_i}}{Q \sum V_i} = \frac{6}{QD[3,2]}$$

Equation 3.4

$D [3,2]$ and $D [4,3]$ consult the surface-weighted mean and volume-weighted mean, respectively. The surface-weighted mean, also known as the Sauter Mean Diameter (SMD), is an average diameter when converted into a sphere, while maintaining the total particle surface area constant. Reactive surface area, viscosity, and hydration reactivity are correlated with this number, which highlights the impact of large surface area particles. The surface area increases and becomes finer as the value decreases. The volume-weighted mean, also referred to as the De Broucker mean, is the volume average diameter of all particles. This value represents the average particle size by volume. Large particles that significantly affect the total volume are emphasized; the more of these there are, the greater the proportion of larger particles and the potential slower hydration reaction.

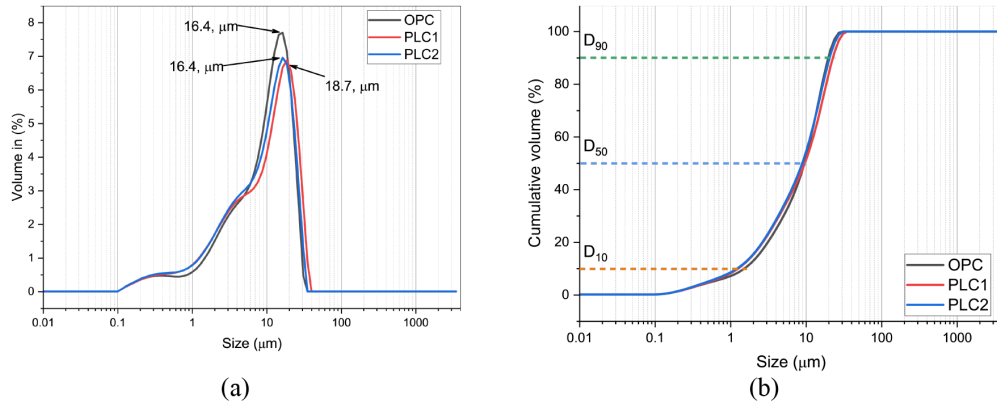


Figure 3.3 Particle Size Distribution of Cements by (a) Volume (%) and (b) Cumulative Volume (%).

TABLE 3.3
Particle Size and Surface Area Characteristics of Cements.

Parameters	OPC	PLC1	PLC2
Span	1.911	2.218	2.161
Uniformity	0.602	0.714	0.691
SSA (m ² /kg)	1975	2078	2165
D [3,2] (μm)	3.04	2.89	2.77
D [4,3] (μm)	11.5	12.4	11.4
D ₁₀	1.76	1.46	1.42
D ₅₀	10.9	11.1	10.2
D ₉₀	22.6	26	23.5

In conclusion, all PLC cements exhibit a generally finer particle size distribution compared to OPC, which can be attributed to the replacement of the clinker with limestone. PLC2 exhibits higher SSA, minor D [3,2], and a more pronounced decrease in D₁₀ compared to OPC, indicating a significant increase in the proportion of fine particles. Furthermore, the uniformity index is 14.7% and 18.6% higher for PLC1 and PLC2, respectively, compared to OPC, suggesting a more uniform particle size distribution. In contrast, PLC1 exhibits a D₉₀ value that is over 15% higher than OPC, indicating a higher proportion of coarse particles, which may reduce its packing effect compared to PLC2.

3.2 Mixture Design

The concrete mixture design used in this work is shown in Table 3.4, and the fine-to-total aggregate ratio is 0.42. Nine concrete mixtures were prepared using OPC, PLC1, and PLC2 cements, with two water reducers. For each mix ID, a total of fifteen 3 × 6-in. cylindrical specimens were cast to measure compressive strength at 1, 3, 7, 14, and 28 curing dates (three specimens per age; ASTM C39/39M-24 [ASTM, 2024d]). Additionally, two 4 × 4 × 16-in. beam specimens were prepared for flexural strength testing at 28 curing dates (ASTM C78/C78M-22; ASTM, 2021b). All concrete specimens were cured in water at 23 °C until the designated test ages. The suggested water reducer dosages for PCE and Lignin are 2–10 oz per cwt (130–650 mL/100 kg) and 2–12 oz per cwt (130–780 mL/100 kg), respectively.

TABLE 3.4
Mixture Proportions of Concrete.

ID	w/c	Cement (lbs/yd ³)	Water (lbs/yd ³)	Fine Aggregate (lbs/yd ³)	Coarse Aggregate (lbs/yd ³)	Water reducer (oz/cwt)	
						PCE	Lignin
OPC							
PLC1						/	/
PLC2							
OPO1-P							
PLC1-P	0.45	564	254	1415	1915	7.7	/
PLC2-P							
OPC-L							
PLC1-L						/	7.7
PLC2-L							

3.3 Fresh and Harden Concrete Properties

3.3.1 Slump Test Result

Figure 3.4 shows the photos of the slump test, which can detect significant differences between those with and without water reducers; these differences are evident in OPC based on the Table 3.5. PCE was most effective in improving the concrete slump, and slump improvement is more effective in the OPC system than in the PLC system.

3.3.2 Setting Time Result

Setting time test run based on the ASTM C403 (ASTM, 2023). PLC1, which has the highest gypsum and alkali content, sets faster than OPC and PLC2. Using a water reducer effectively retards the setting of OPC and PLCs. Additionally, it increases the duration between the initial and final settings of OPC while shortening the duration of PLC.

3.3.3 Isothermal Calorimetry Test Result

Isothermal calorimetry (IC) tests were performed on a cement paste with a water-to-cement (w/c) ratio of 0.45 at 23 °C in Figure 3.6. Since PLC1's sulfate is mostly provided



Figure 3.4 Photos of the Slump Test.

TABLE 3.5
Slump Values of Different Mixtures (Data in Brackets is the Slump Increase Compared to the Plain Mixture).

	Plain	PCE	Lignin
OPC	0.5"	6.75" (+ 6.25")	4.25" (+ 3.75")
PLC1	2"	7.1" (+ 5.1")	5.25" (+ 3.25")
PLC2	2.1"	7.5" (+ 5.4")	3.5" (+ 1.4")

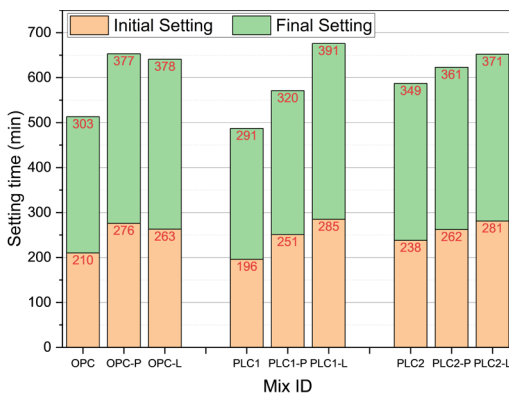
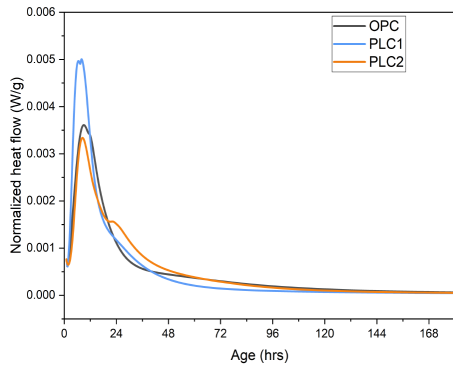


Figure 3.5 The Setting Time of Different Concrete Mixtures.

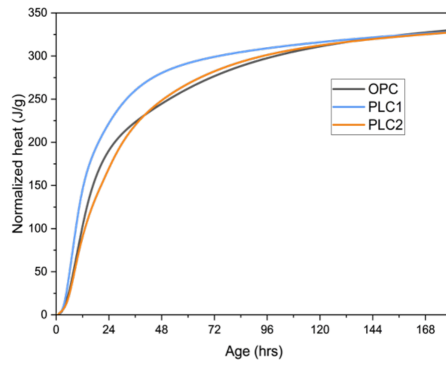
as alkali sulfate instead of gypsum, it causes early accumulation of sulfate and alkali in the pore solution, which intensifies the reactions of aluminates (Andrade Neto et al., 2021). Therefore, this results in high early-age heat release. PLC2 exhibits a secondary hydration heat peak at approximately 24 hr, which can be attributed to the formation of monosulfate (Afm) ($C_3A + Aft = Afm$). OPC and PLC2 have a higher belite (C_2S) content than PLC1, resulting in greater heat release after 7 days.

Figure 3.7 presents the heat flow of all mixtures. It is found that adding water reducers slightly increases the peak heat flow of OPC and slightly delays the peak time. For PLC1, adding water reducers reduces the peak heat flow and delays its onset. For PLC2, adding water reducers significantly increases the peak heat from Afm generation, especially with the PCE water reducer, which further amplifies this peak.

Figure 3.8 plots the total released heat of all mixtures. It is found that adding water reducers increases the total heat released from OPC. Water reducers slightly reduce the total heat released from PLC1. The PCE water reducer increases the heat released from PLC2, and the Lignin water reducer also slightly increases the total heat released by PLC2.



(a) Heat Flow



(b) Total Released Heat

Figure 3.6 IC Test Results of Plain Mixtures Without Water Reducers.

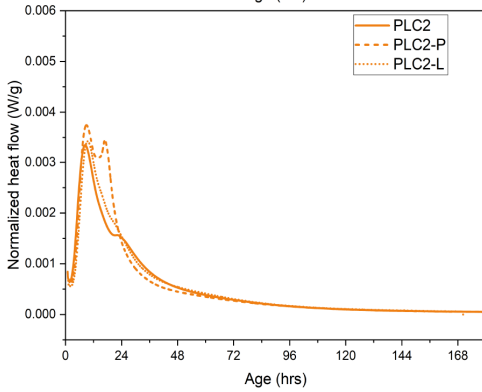
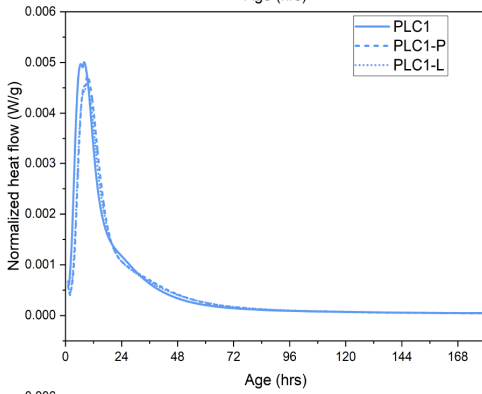
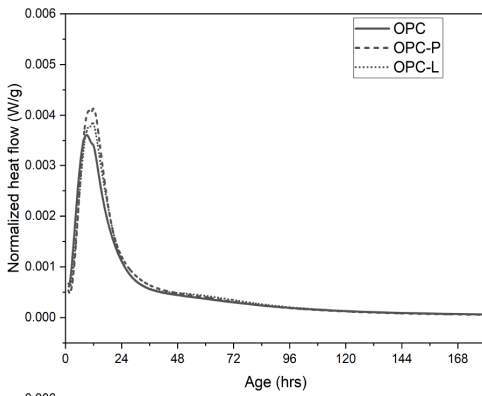


Figure 3.7 The Heat Flow of All Mixtures.

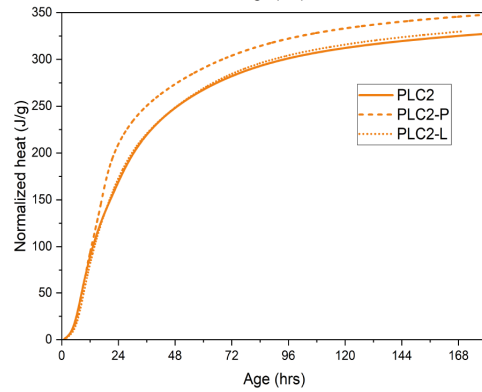
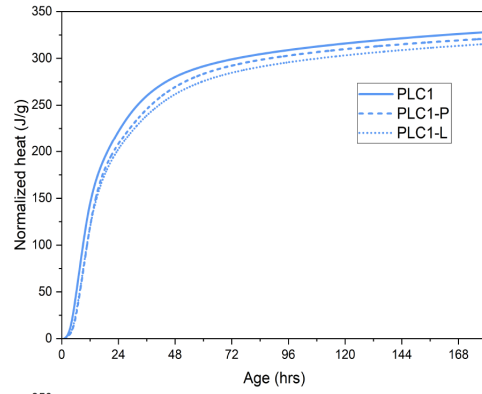
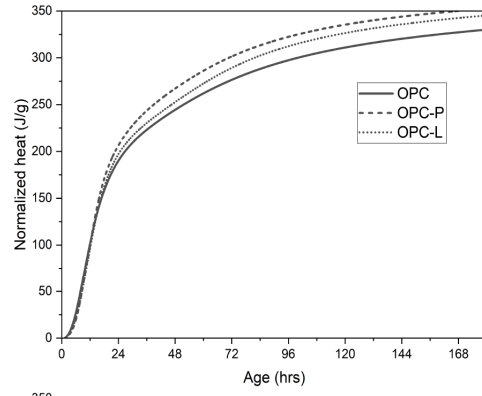


Figure 3.8 Total Released Heat of All Mixtures.

3.3.4 TGA results

The TGA was performed on all the mixtures from 1 to 28-day age, and the CH content, also known as Portlandite, is determined, as shown in Figure 3.9. Generally, adding water reducers slightly reduces CH generation at early ages. Nevertheless, this reduction in CH content becomes less obvious at later ages. PCE water reducer does not significantly affect the hydration degree as the lignin water reducer does.

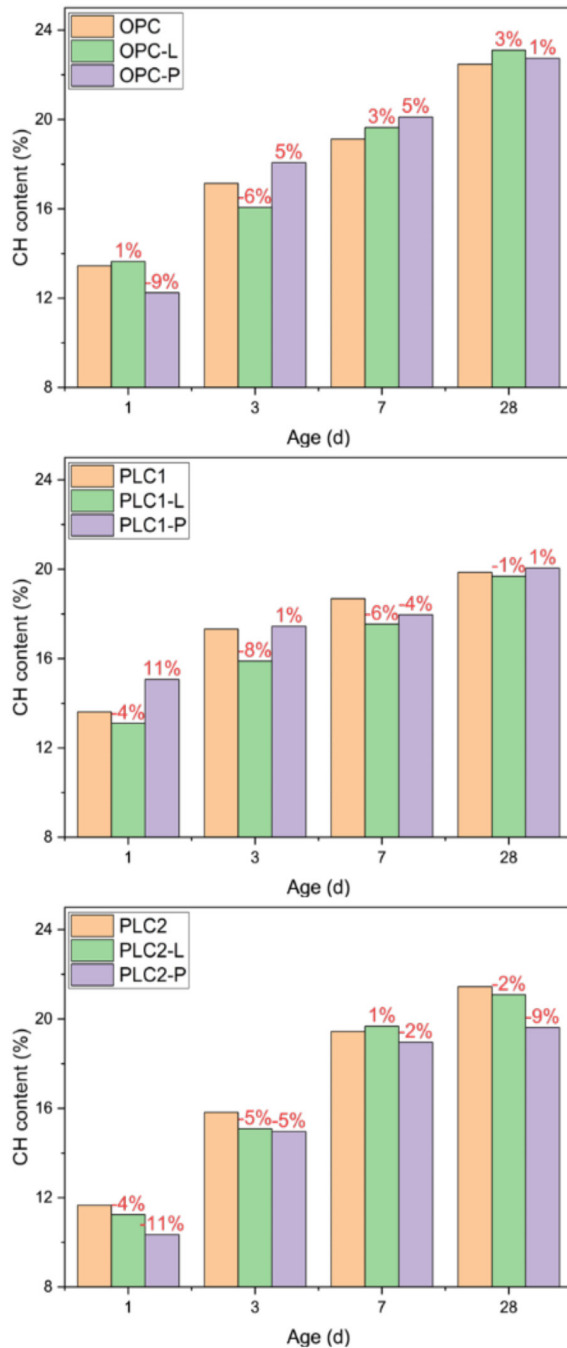


Figure 3.9 Calcium Hydroxide (CH) Content Determined by TGA Analysis.

3.3.5 Shrinkage Test

Shrinkage tests have been performed using a mortar bar in 50% relative humidity (RH) and 100% RH curing conditions at 23 °C, as field operations observed low flexural strength due to shrinkage cracks in PLC concrete. Through Figure 3.10, 100% RH curing conditions, in which the mixtures are water-saturated, demonstrated a relatively lower shrinkage percentage than 50% RH conditions. PLC1 showed the highest shrinkage percentage

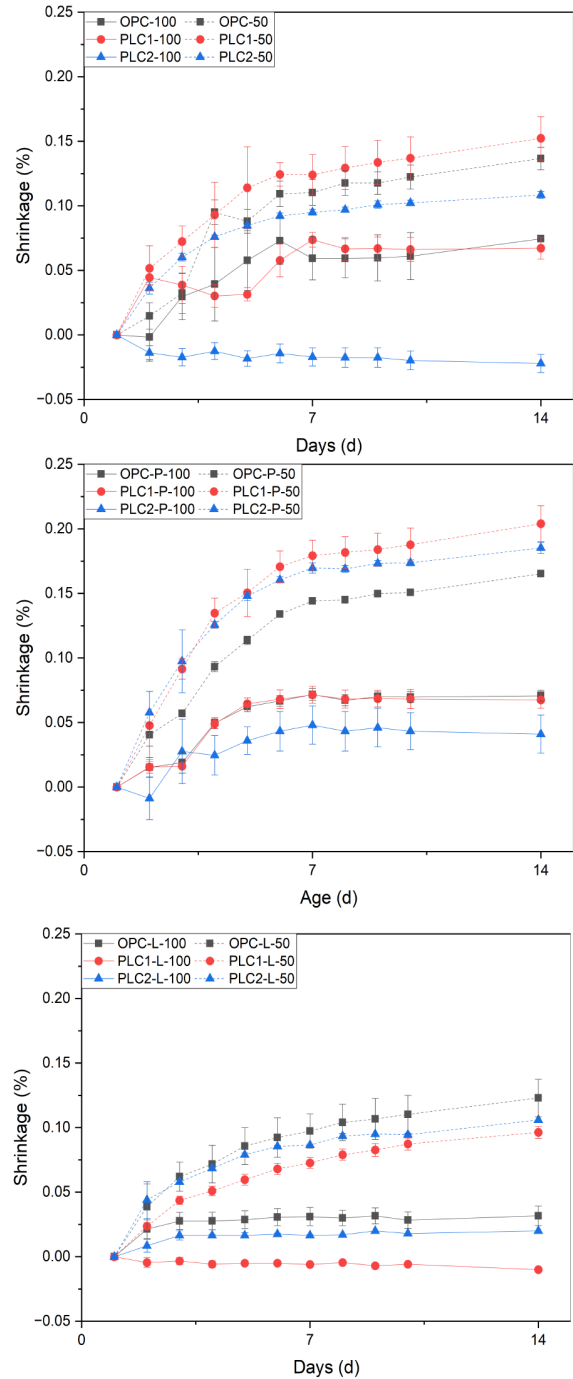


Figure 3.10 Shrinkage of All Mixtures at 50% RH and 100% RH.

in both conditions without water reducers, while PLC2 had the lowest. However, when the mortar was mixed with the Lignin water reducer, PLC1 exhibited the lowest shrinkage in both conditions, and all cases showed lower shrinkage than those without a water reducer or with the PCE water reducer.

3.4 Mechanical Properties

3.4.1 Compressive Strength

Figure 3.11 plots the compressive strength development of all concrete mixtures. PLC1 concrete showed less strength loss than PLC2 concrete throughout the 28-day curing period. While

PCE concrete (except for PLC2) exhibits strengths equivalent to those of concrete without a water reducer, lignin concrete continues to exhibit decreased compressive strength at a later age. Figure 3.12 shows how concrete with the same composition, but different cements, develops in terms of compressive strength. While PLC1 initially displays greater strength than PLC2, this trend reverses after 3 or 7 days of curing. This phenomenon occurs due to the difference in gypsum and belite content detected by QXRD. The hydration of PLC1, especially alite (C_3S), can be accelerated because it contains the highest gypsum content. This reaction may increase the early-age strength of the concrete. Additionally, OPC consistently demonstrates the highest compressive strength across all combinations.

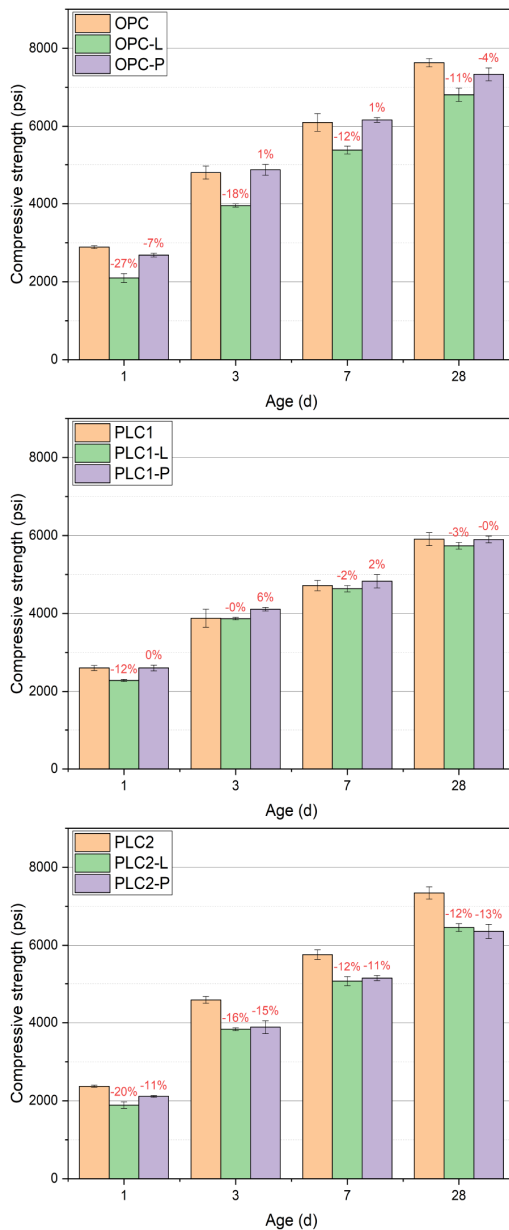


Figure 3.11 Comparison Graph of the Compressive Strength of All Mixtures With Different Water Reducers.

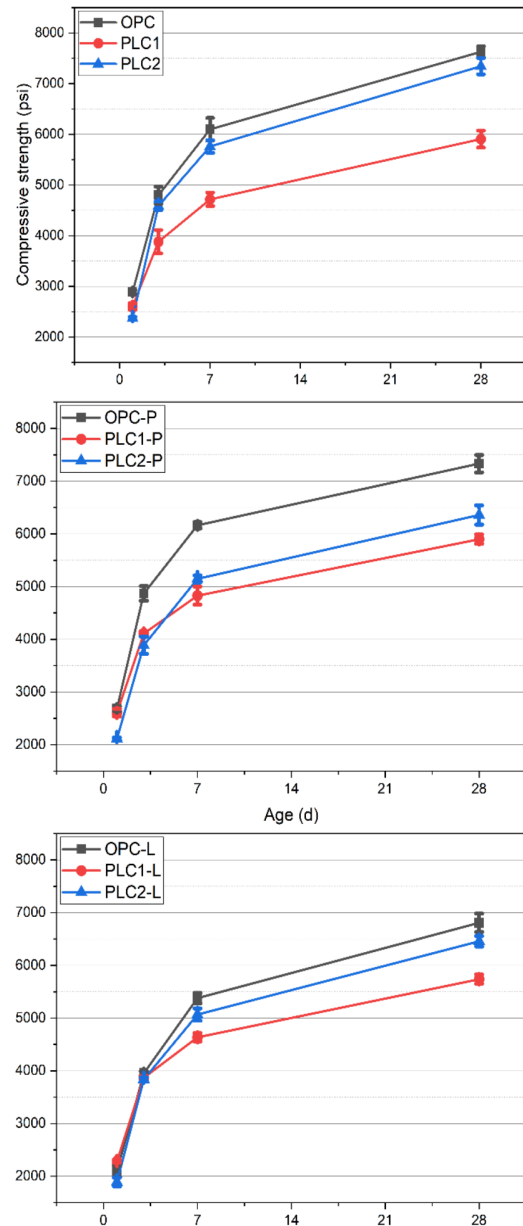


Figure 3.12 Comparison of Compressive Strength Development in Different Cement Systems.

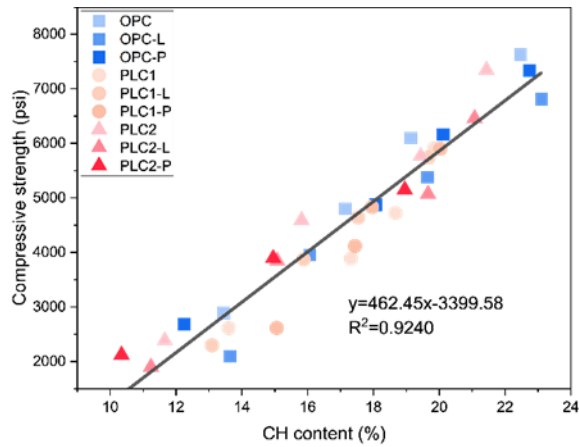


Figure 3.13 Compressive Strength in Terms of CH Content.

Figure 3.13 plots the relationship between compressive strength and CH content, as well as hydration degree. The CH content and compressive strength exhibit a unified relationship for all mixtures, indicating that the CH content (associated with C-S-H formation) dominates the strength development of OPC and PLC concrete (without SCMs). However, the relationship between strength and hydration degree indicates that at the same degree of hydration, OPC concrete has a higher compressive strength than PLC concrete. At an early age, PLC1 concrete exhibits higher compressive strength, whereas PLC2 concrete shows faster development of compressive strength.

3.4.2 Flexural Strength

Figure 3.14 plots the flexural strength of all mixtures at 28 days of curing. It is worth noting that all concrete specimens were cured in water at 23 °C. In general, OPC concrete has the highest flexural strength when no water reducers are used. The flexural strength of all mixes is marginally increased using water reducers, in contrast to compressive strength. In PLCs, this growth is more notable.

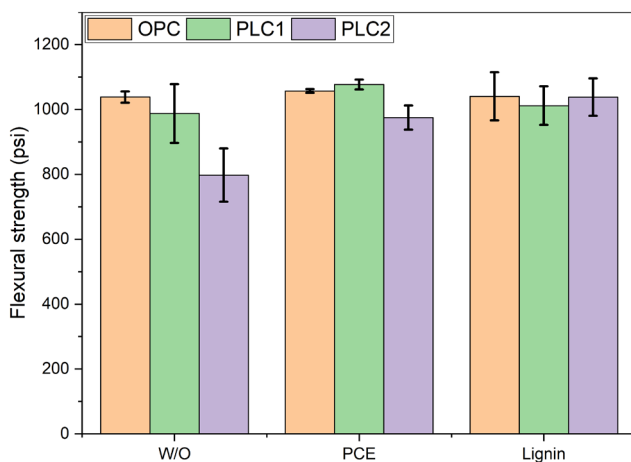


Figure 3.14 Flexural Strength of All Mixtures at 28 Days of Curing.

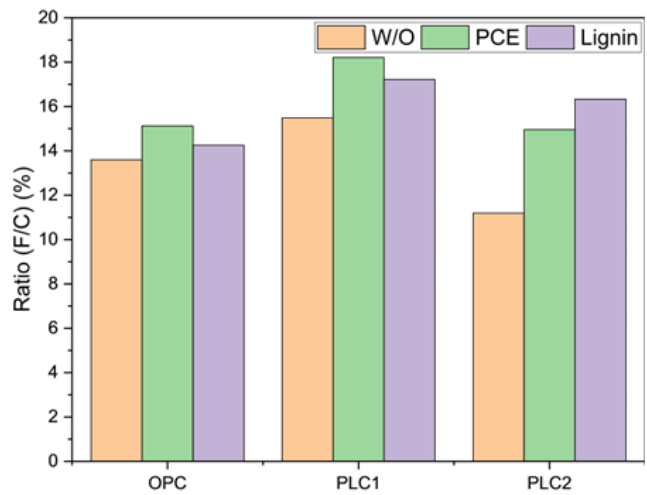


Figure 3.15 Flexural-to-Compressive Strength Ratio of All Mixtures.

Figure 3.15 plots the flexural-to-compressive strength ratio of all mixtures at 28 days of curing. The ratios of OPC mixtures are all lower than those of PLC mixtures because of their strong compressive strength. The ratio rises when water reducers are added, which is explained by a little gain in flexural strength but a decrease in compressive strength.

3.5 Durability Properties

3.5.1 Bulk and Surface Resistivity Test Result

Bulk resistivity has been measured according to ASTM C1876 through various curing dates to track the change in resistivity in Figure 3.16 (ASTM, 2024c). Notably, even with or without water reducers, the resistivity of PLC1 exceeded that of OPC and PLC2 at early ages (3 and 7 days), and development was sustainable, which shows the highest resistivity at 28 curing days. Sersale et al. (1991) reported that the proper content of gypsum in cement can densify the microstructure. When the cement contains more than 2.5% sulfur trioxide content, the intensity of pore size distribution gradually shifts to less than 1000 Å at 28 days of curing (Sersale et al., 1991). This phenomenon also occurred in the surface resistivity test in Figure 3.17, which followed AASHTO T358 (AASHTO, 2019). Still, PLC1 had the highest resistivity after 28 days of curing; however, none of the cases could reach or exceed the moderate chloride ion penetration limit (> 12kΩcm). Simple trends in electrical resistivity, particularly at early ages when saturation heavily influences the signal, are inadequate for a dependable assessment of concrete durability (He et al., 2023). Therefore, the vacuum-saturated formation factor, applying a pore-solution conductivity correction, has been calculated to account for both porosity and pore connectivity as a complementary analysis.

Using the National Institute of Standards and Technology (NIST)-estimated pore solution conductivity, the vacuum-saturated formation factor, defined as bulk resistivity divided by pore-solution resistivity, was determined and used as an

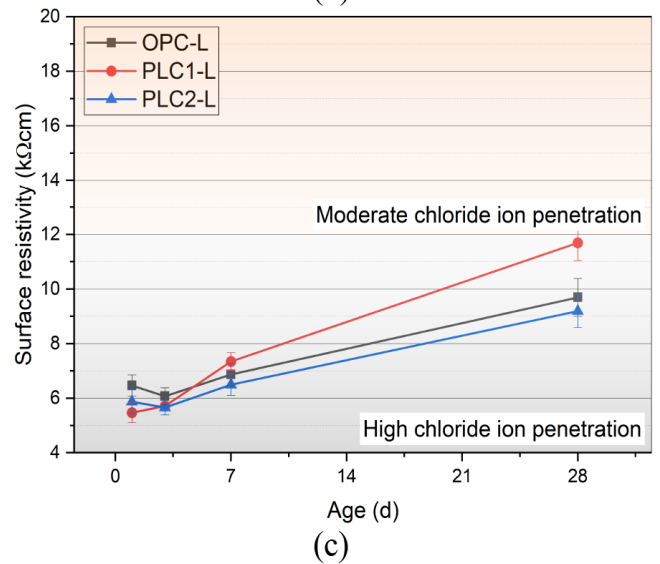
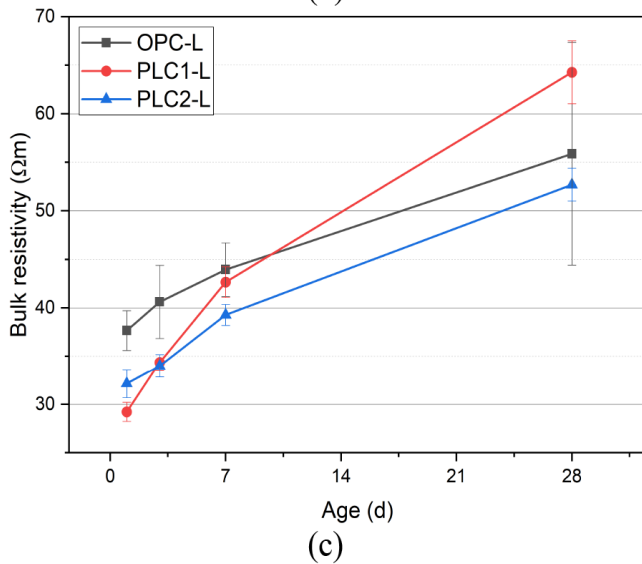
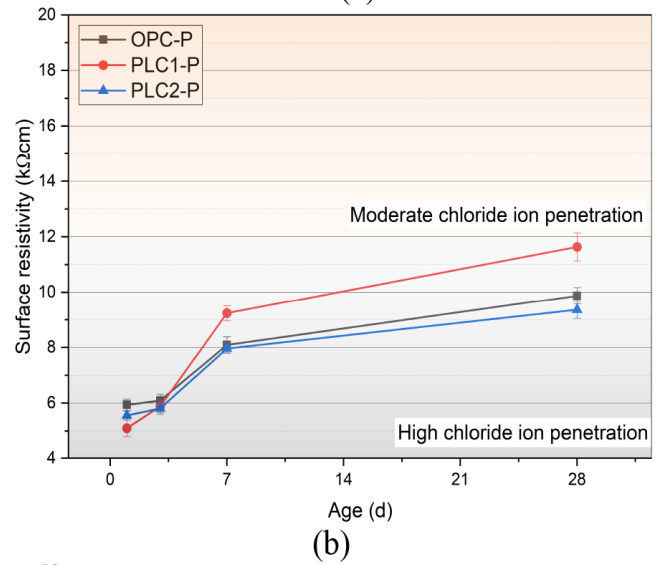
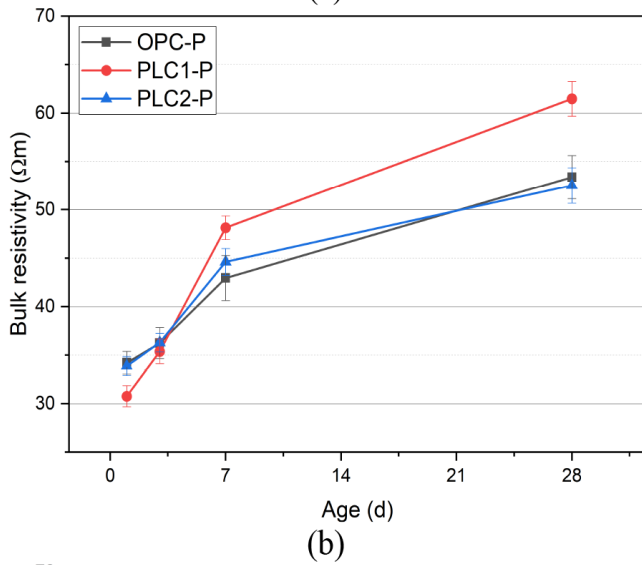
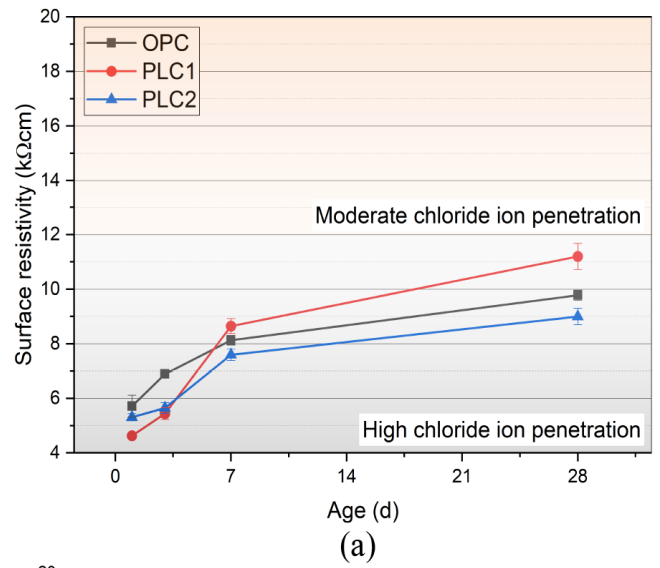
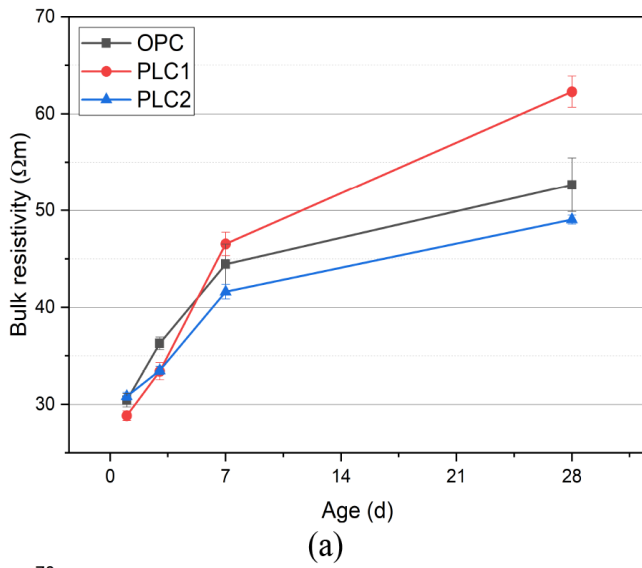


Figure 3.16 Comparison Graph of the Bulk Resistivity Results of All Mixtures.

Figure 3.17 Comparison Graph of the Surface Resistivity Test Results of All Mixtures.

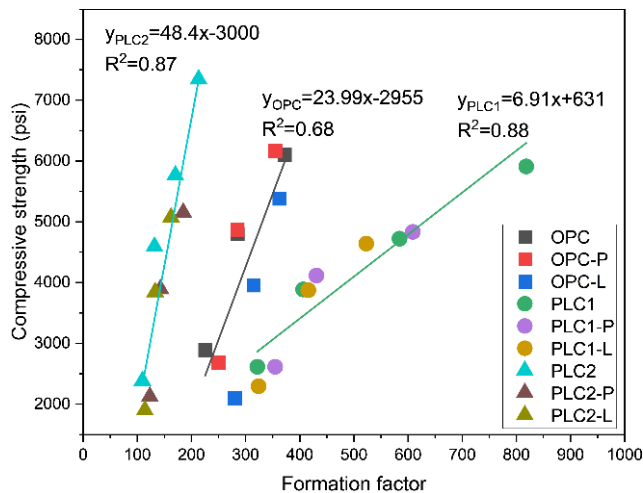


Figure 3.18 Formation Factor in Terms of Compressive Strength.

indirect index of ion transport, capturing both porosity and pore connectivity (Banik et al., 2024). Figure 3.18 plots the relationship between formation factors and compressive strength. The high alkaline and gypsum content of PLC1 alters the pore solution chemistry, resulting in low resistivity at an early age. With the same formation factor, PLC2 exhibits the highest compressive strength, attributed to alite and belite. In contrast, PLC1 has the lowest compressive strength due to its low belite content and abundant Aft and Afm formation resulting from gypsum.

3.5.2 Void Content Result

The void content of the samples was calculated based on ASTM C642 (ASTM, 2021a); however, the water vacuum saturation method was used to determine the apparent mass of the sample in water after immersion and boiling (D) at the highest level of vacuum (7Torr) which is very similar to the theoretical maximum porosity of the concrete, as described by Bu et al. (2014).

In Figure 3.19, PLC1 had the lowest void content among the others in the condition without water reducers and still showed a comparable result with OPC with water reducers. PLC2 always had the highest void content in all cases.

3.5.3 Water Absorption Test Result

The water absorption test is performed under ASTM C1585; all concrete samples are 28 days cured and dried in a 50 °C oven for 72 hr (ASTM, 2020). When adding water reducers, PLC2 concrete exhibits the highest sorptivity (I) compared to the others, whereas OPC concrete has the highest sorptivity without water reducers. PLC1 concrete had a similar or lower initial absorption rate than the others but demonstrated the lowest secondary absorption rate. This means that PLC1 concrete has small radius capillary pores and a complex pore structure; however, this result can be further explained by

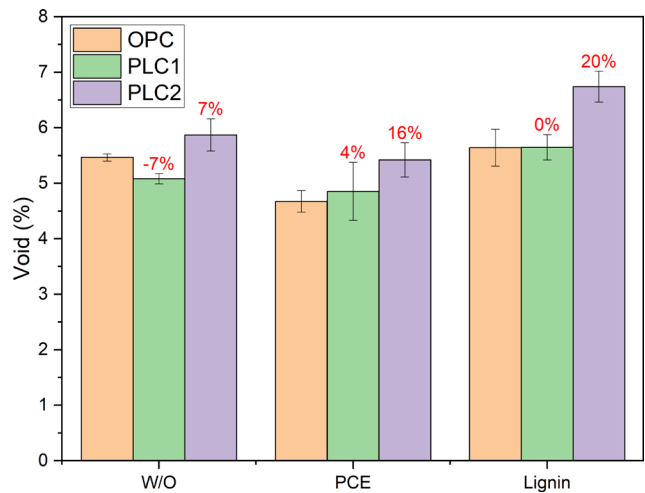


Figure 3.19 Comparison Graph of the Void Content Results Based on the Water Reducers (28 Days).

the assumption that capillary pores are cylindrical. Without a water reducer, OPC concrete is estimated to have the highest sorptivity in long-term absorptions and the highest rate in both initial and secondary absorptions.

These results have also been confirmed in other studies. According to the study by Nadelman and Kurtis (2019), PLC mortar exhibited lower initial water absorption than OPC mortar at a 0.4 water-to-binder (w/b) ratio. In addition, Tennis et al. (2011), citing the work of Tsivilis et al. (2003), reported that PLC concrete shows reduced water permeability and lower sorptivity. Thus, it can be concluded that the three primary mechanisms by which limestone contributes to PLC performance are increased concrete density and improved pore structure, which aligns with the result.

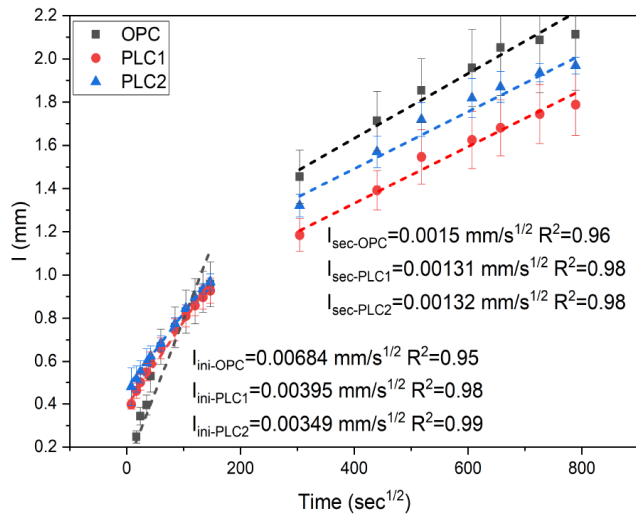
3.5.4 RCPT Result

Figure 3.21 demonstrates the result of the Rapid Chloride Penetration Test (RCPT) based on ASTM C1202 (ASTM, 2022). All the mixtures fall within the range of moderate chloride ion penetrability (2000~4000 coulombs) and align with other test results. PLC1 had the lowest penetration in all cases, which can be attributed to the dense and complex microstructure of PLC1 concrete, making it difficult to penetrate.

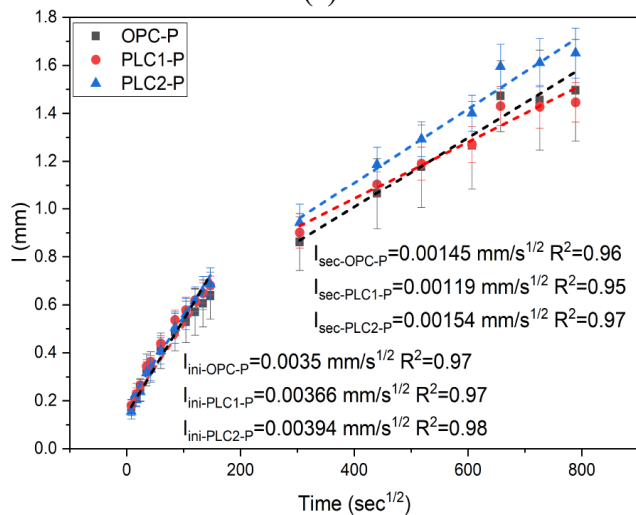
3.6 Summary

This section evaluated the physical and chemical properties of three different cements, as well as the performance of fresh and hardened concrete, with a focus on identifying the changes that occur when a water reducer is added.

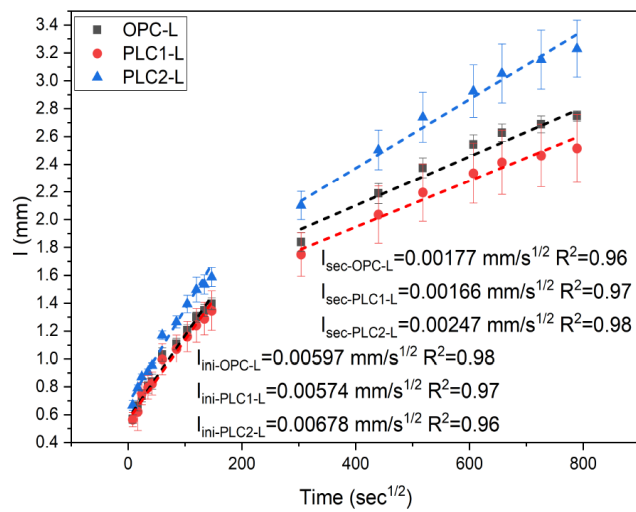
The higher gypsum content in PLC1 was the key factor that led to significantly different performance compared to the others. Since the appropriate gypsum content accelerates the hydration of the alite, PLC1 concrete exhibited relatively high early-age strength and higher resistance to chloride ion penetration. Additionally, due to the smaller radius of capillary pores and dense microstructure,



(a)



(b)



(c)

Figure 3.20 Water Absorption Test Result With Initial Absorption Rate (I_{ini}) and Secondary Absorption Rate (I_{sec}).

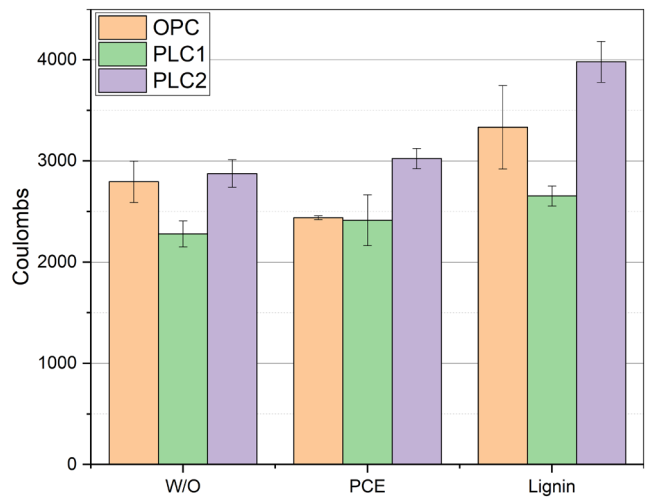


Figure 3.21 RCPT Result of All Mixtures.

it exhibited a faster or similar initial absorption rate (I_{ini}) and a slower secondary absorption rate (I_{sec}) compared to the other mixtures. Nevertheless, PLC1 exhibits inferior long-term compressive strength compared to OPC due to its low belite content.

By adding water reducers, all mixtures showed the retard effect of setting and reaction heating flow through the setting time test and IC test. Additionally, the compressive strength of PLC2 concrete decreased significantly with the use of water reducers, but the flexural strength increased; meanwhile, other cements did not show a substantial difference between those with and without water reducers.

Through the durability test, PLC1 concrete has the densest microstructure among the others, despite having the lowest compressive strength. This can be explained by the high content of gypsum in PLC1. Gypsum generates Aft by reacting with C_3A and accelerates the hydration of alite at the early stage, allowing it to fill the space before it sets. However, as Aft does not support building the strength of concrete and PLC1 has a lower belite content, it is unlikely that PLC1 concrete can exhibit higher compressive strength than the others.

4. ITZ EVALUATION THROUGH SCANNING ELECTRON MICROSCOPE SEM-BSE IMAGE ANALYSIS

The ITZ is the critical area between the cement paste and the aggregate. It is widely accepted that this region is formed due to the wall effect, which occurs before the concrete sets. As cement grains are repelled from the aggregate surface, the local w/c ratio near the aggregate increases due to the physical characteristics of the cement grains. This results in the formation of a zone with high porosity once the setting is complete and moisture has evaporated, weakening the ITZ's physical properties.

Given that the ITZ typically exhibits a higher porosity than the bulk cement paste, SEM-BSE imaging, has been employed to quantify the microstructural properties of the ITZ. This technique has been widely adopted in various studies. This chapter compares the ITZ properties of various cements and assesses how these differences impact mechanical strength.

4.1 Image Analysis Process

The process of the BSE image analysis is divided into six steps, which are shown in Figure 4.1.

4.1.1 Image Collection and Preprocessing

The analysis method utilizes 8-bit grayscale images to perform binary segmentation, separating porous and nonporous areas (fine aggregates or bulk paste). Porosity variations are then measured at regular distance intervals from the aggregate boundary to define the thickness and porosity of the ITZ. BSE images were acquired at 2000× magnification using a Thermo Fisher™ Apreo™ 2 SEM, with a resolution of 67.65 nm (0.0068 μm) per pixel, ensuring high image fidelity and detail. Thirty images were taken for each sample to ensure reliability and stable results. Aggregate boundaries were manually identified using ImageJ and assigned a grayscale value of 255 (white). To avoid misclassification during subsequent analysis, any existing pixels with a value of 255 in the original image were preprocessed and adjusted to 254.

4.1.2 Defining Breakpoint and Strip Delineation

According to previous studies, the threshold value for pore regions in this image analysis has traditionally been determined using the overflow criterion (Gao, De Schutter, Ye, Huang, et al., 2013; Gao, De Schutter, Ye, G., Tan, & Wu, 2014; Lyu et al., 2019; Wu et al., 2016). This criterion defines the threshold based on the inflection point in a cumulative grayscale value vs. pixel count curve, specifically, the point where the curve transitions from a gradual to a steep increase, marking the boundary between pores and bulk paste (Wong et al., 2006). However, as noted in the literature, this approach tends to overestimate

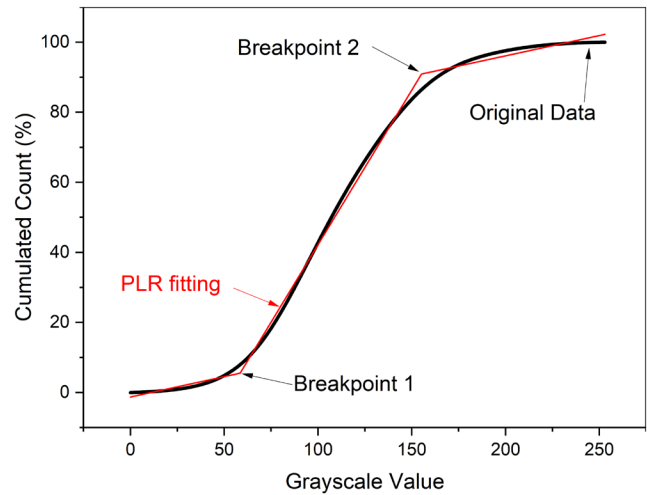


Figure 4.2 The Example Graph for the Application of PLR.

the threshold and lacks a consistent definition for the transition range, introducing potential for human error.

To address these limitations, we employed a statistical technique known as Piecewise Linear Regression (PLR) to automate the analysis and ensure consistency. PLR identifies breakpoints in data by fitting two or more linear models and has been widely applied across various fields (McZgee & Carleton, 1970). Figure 4.2 shows the schematic applied example to the cumulative count graph of the BSE image. The first breakpoint (Breakpoint 1 in Figure 4.2) was defined as the threshold between pore regions and bulk paste.

In the subsequent step, strip delineation was performed using Euclidean distance mapping, as proposed by Wong and Buenfeld (2006). As shown in Figure 4.3, aggregate boundaries were offset at regular intervals of 5 μm, generating 10 concentric

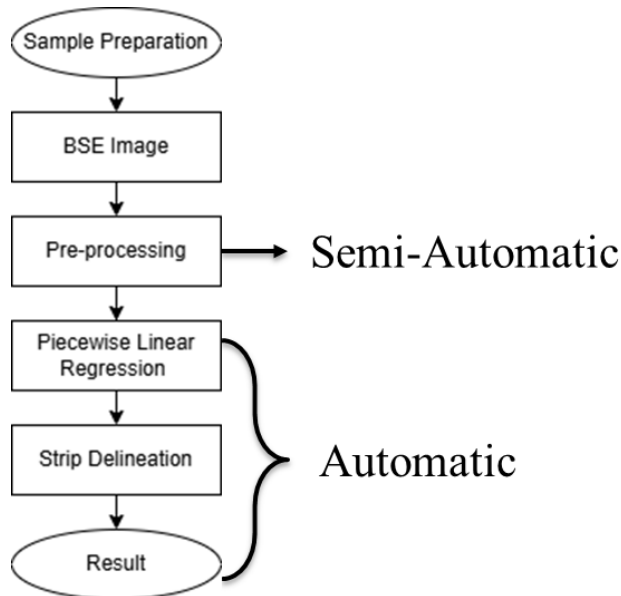


Figure 4.1 Flowchart of Analysis Method for Defining ITZ Thickness.

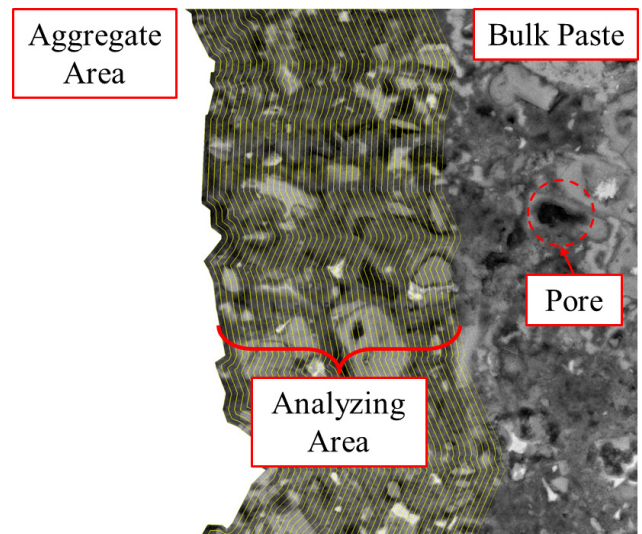


Figure 4.3 The Example of the BSE Image with Strip Delineation.

zones extending to 50 μm from the aggregate interface. This setting was chosen based on the commonly accepted ITZ range, which spans approximately 10–50 μm (Scrivener et al., 2004). After completing both steps, the image was binarized using the PLR-derived threshold value. The porosity of each zone was then calculated based on this binarized image.

4.1.3 Porosity Result

The result of the porosity distribution through the distance from the aggregate is demonstrated in Figure 4.4. In most cases, PLC concretes exhibited thinner ITZ thicknesses than OPC concretes, which can be attributed to the filler effect. Interestingly,

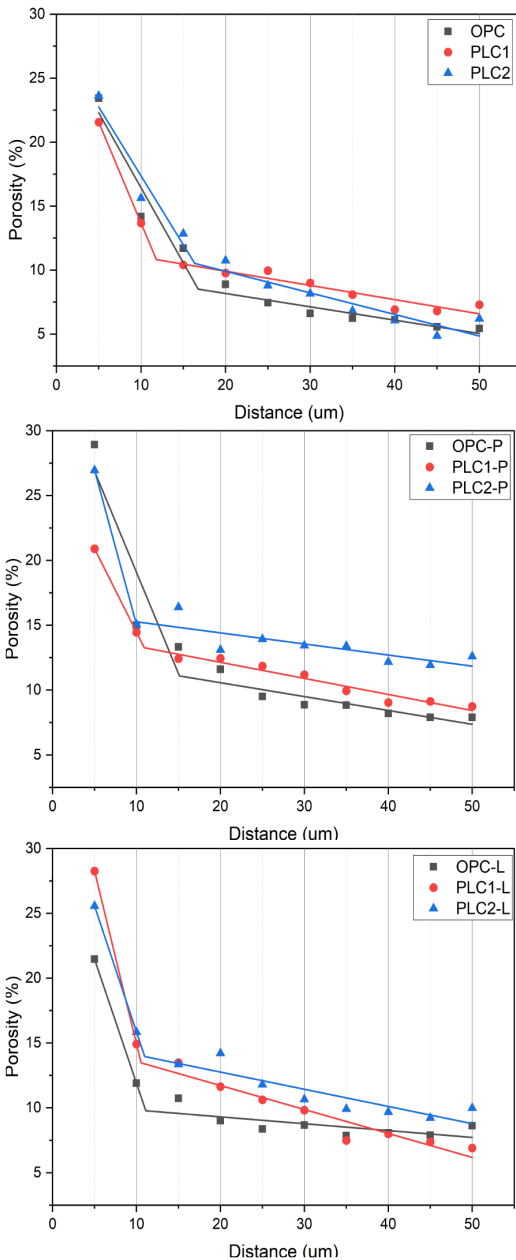


Figure 4.4 ITZ Porosity Analysis Results.

TABLE 4.1
The Estimated Thickness of the ITZ.

	ITZ (μm)
OPC	16.76 \pm 1.55
PLC1	11.81 \pm 0.57
PLC2	16.35 \pm 1.74
OPC-P	15.12 \pm 1.84
PLC1-P	10.92 \pm 0.5
PLC2-P	9.9 \pm 0
OPC-L	11.10 \pm 0.57
PLC1-L	10.54 \pm 0.42
PLC2-L	10.97 \pm 0.73

TABLE 4.2
The Average Porosity of the ITZ.

	Ave. Porosity (%)		
	OPC	PLC1	PLC2
WO	16.44	17.62	17.37
PCE	19.08	17.68	21.01
Lignin	16.68	21.59	20.71

by adding the water reducers, all concretes showed a decrease in thickness, but an increase in average porosity of the ITZ. This result aligns with Xu and Beaudoin’s (2000) work which claims that the ITZ thickness has been improved by adding a PCE water reducer. However, even though the water reducers enhance the porosity and thickness, the compressive strength of the PLC1 with water reducers was the lowest, especially with the PCE water reducer. This result can be attributed to the CH content surrounding the aggregate.

4.2 CH Content

The element map around the aggregate surface is shown in Figure 4.5; it is found that the PLC1 concrete with PCE water reducer has a high CH accumulation around the aggregate surface. This phenomenon has also been reported by Diamond and Haug (2001). The 0 to 5 μm area around the aggregates could have lower porosity because the CH is dominant than the pores. Figure 4.6 plots the CH content around the aggregate surface. It was observed that with PCE, all PLCs exhibited a considerable accumulation of CH around the aggregates, with PLC1 showing a significantly high concentration around the aggregate. As CH is a weak and brittle hydration product, it contributes little to the overall strength of concrete. Thus, it was found that PLC1’s lower compressive strength, despite having an ITZ with low porosity, was due to its high CH content.

4.3 Summary

This section focuses on quantitatively studying the physical properties of the ITZ, including its thickness and porosity, through BSE image analysis. CH distribution analysis was conducted through additional image analysis to resolve the discrepancy between compressive strength and ITZ properties evaluation.

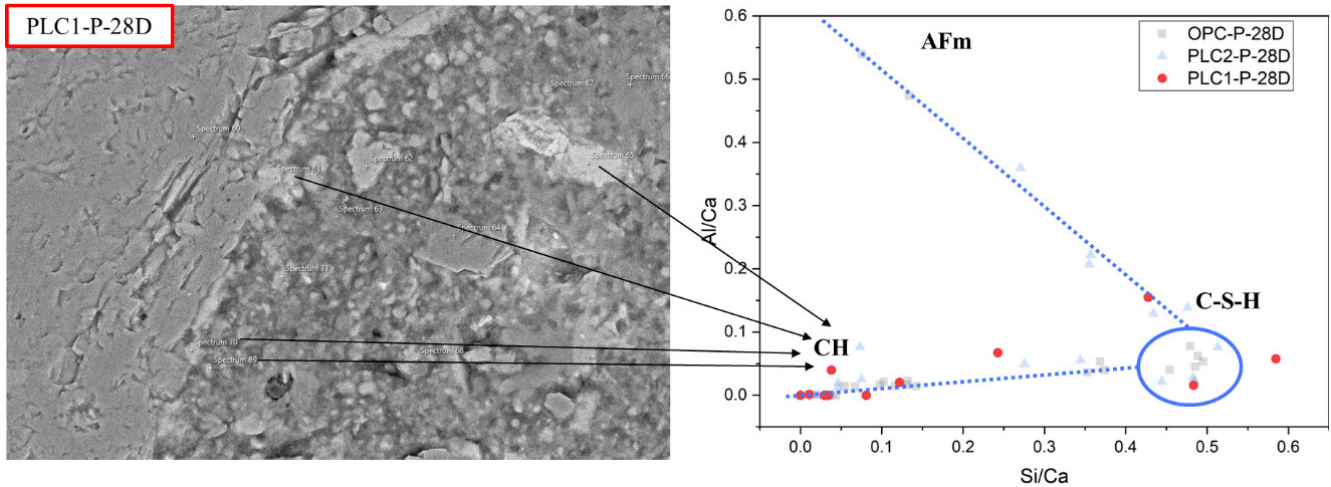


Figure 4.5 Element Distribution Around the Aggregate.

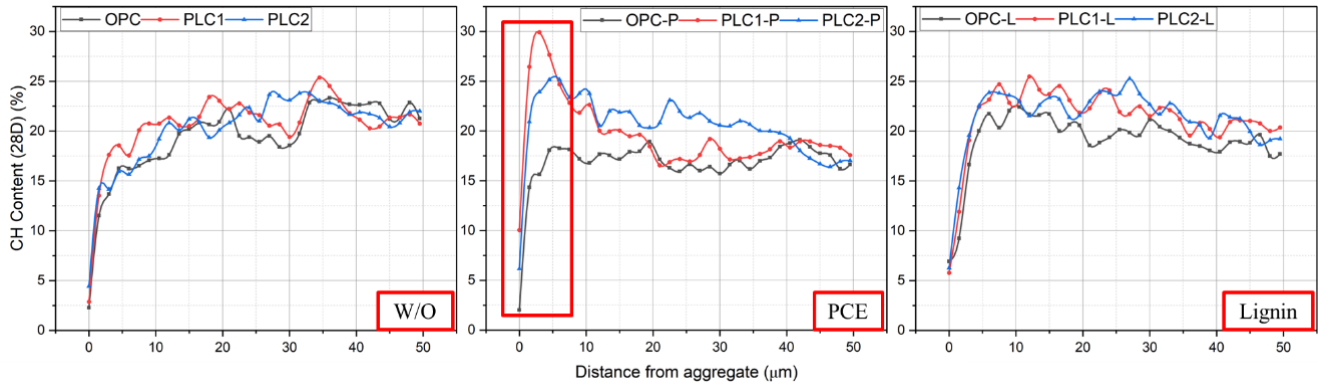


Figure 4.6 CH Content Around the Aggregate Surface.

The first section of all mixtures was set at 4.5 μm , and we can assume that all the cement has the same particle size. The second section exhibits a gradual trend compared to the first section, but a more rapid trend than the bulk paste. Thus, this result suggests that the ITZ may be divided into two sections.

By adding water reducers, the ITZ thickness of the OPC and PLC2 concretes increased significantly. On the other hand, the ITZ thickness of PLC1 concrete had decreased. However, the ITZ thickness result obtained from strip delineation was probably underestimated because the PLC1 found that adding PCE water reducer to the mix reduces porosity around the aggregate. Thus, these results suggest that in this instance, it is necessary to thoroughly assess the ITZ's characteristics by looking at its CH content.

5. FINAL CONCLUSIONS AND RECOMMENDATIONS

5.1 Conclusions

This study presents a comprehensive evaluation of two commercially available PLC systems compared to OPC for use in structural and pavement-grade concrete mixtures. The investigation

included detailed material characterization, mechanical and durability performance testing, and advanced microstructural analysis with a particular focus on the ITZ. The following key conclusions are drawn:

- *Material Variability Influences Performance:* Commercial PLCs exhibit variability in mineralogy, gypsum content, limestone fineness, and alkali levels. These differences influence hydration kinetics, mechanical strength development, and durability performance.
- *Early-Age Strength and Durability Trade-offs:* PLC1, characterized by high gypsum and alkali content, exhibited improved early-age strength and chloride resistance due to rapid hydration and a refined pore structure. However, its long-term compressive strength was limited by low Belite content and CH accumulation in the ITZ. In contrast, PLC2 demonstrated a more balanced strength gain over time and better flexural performance.
- *Impact of Water Reducers:* The type of water-reducing admixture significantly influenced hydration behavior and ITZ characteristics. PCE improved workability but increased ITZ porosity and promoted CH accumulation around aggregates in PLC1, which adversely affected compressive strength. Lignosulfonate showed lower shrinkage but did not significantly improve long-term mechanical performance.

- *Durability Assessment Confirms Microstructural Trends:* Durability indicators, such as surface and bulk resistivity, void content, water absorption, and RCPT, are aligned with microstructural observations. PLC1 consistently exhibited higher resistivity and lower chloride ion penetration, consistent with a denser matrix, yet this did not correlate with higher mechanical strength due to its weaker ITZ.
- *ITZ Properties Are Critical to Performance:* BSE image analysis revealed that PLCs generally form thinner ITZs due to the filler effect. However, ITZ porosity and CH content—especially when modified by admixtures—play a more critical role than thickness alone in determining mechanical strength. Excessive CH near aggregate surfaces compromises ITZ integrity despite low porosity readings.

5.2 Recommendations

Based on the findings of this study, the following recommendations are proposed for engineers, materials suppliers, and transportation agencies considering the use of PLC in infrastructure applications:

- *Adopt Performance-Based Specifications:* Rather than prescriptive cement replacement levels, performance-based criteria should be emphasized—especially for strength, shrinkage, and chloride resistance. Specifications should require prequalification of PLC sources with representative admixture combinations.
- *Tailor Mix Designs by PLC Source:* Due to the variability in PLC properties, mix designs should be customized to the specific cement source. Factors such as gypsum content, limestone fineness, and alkali levels must be considered when selecting admixtures and determining mix proportions.
- *Select Water Reducers Judiciously:* Admixture compatibility is crucial. PCEs should be used cautiously with PLCs that already contain high gypsum or alkali content to avoid excessive CH formation. Alternative admixtures or lower dosages may mitigate adverse ITZ effects.
- *Encourage Microstructural Evaluation for High-Performance Applications:* For critical infrastructure or high-performance concrete, agencies and researchers are encouraged to include ITZ evaluation using techniques such as SEM-BSE and TGA to gain insights into long-term durability behavior.
- *Promote Broader Adoption with Technical Support:* While PLC offers significant carbon reduction potential, its successful implementation requires technical guidance and training. State DOTs and industry organizations should disseminate best practices and case studies to support wider adoption.

REFERENCES

- American Association of State Highway and Transportation Officials. (2019). *Standard method of test surface resistivity indication of concrete's ability to resist chloride ion penetration* (AASHTO T358-19). American Association of State Highway and Transportation Officials.
- Andrade Neto, J. d. S., De la Torre, A. G., Kirchheim, A. P. (2021). Effects of sulfates on the hydration of Portland cement – A review. *Construction and Building Materials*, 279, 122428. <https://doi.org/10.1016/j.conbuildmat.2021.122428>
- ASTM International. (2020). *Standard test method for measurement of rate of absorption of water by hydraulic-cement concretes* (ASTM C1585-20). <https://doi.org/10.1520/C1585-20>
- ASTM International. (2021a). *Standard test method for density, absorption, and voids in hardened concrete* (ASTM C642-21). <https://doi.org/10.1520/C0642-21>
- ASTM International. (2021b). *Standard test method for flexural strength of concrete (using simple beam with third-point loading)* (ASTM C78/78M-22). https://doi.org/10.1520/C0078_C0078M-22
- ASTM International. (2022). *Standard test method for electrical indication of concrete's ability to resist chloride ion penetration* (ASTM C1202-22). <https://doi.org/10.1520/C1202-22>
- ASTM International. (2023). *Standard test method for time of setting of concrete mixtures by penetration resistance* (ASTM C403/403M-23). https://doi.org/10.1520/C0403_C0403M-23
- ASTM International. (2024a). *Standard specification for blended hydraulic cements* (ASTM C595/595M-24). https://doi.org/10.1520/C0595_C0595M-24
- ASTM International. (2024b). *Standard specification for portland cement* (ASTM C150/C150M-24). https://doi.org/10.1520/C0150_C0150M-24
- ASTM International. (2024c). *Standard test method for bulk electrical resistivity or bulk conductivity of concrete* (ASTM C1876-24). <https://doi.org/10.1520/C1876-24>
- ASTM International. (2024d). *Standard test method for compressive strength of cylindrical concrete specimens* (ASTM C39/39M-24). https://doi.org/10.1520/C0039_C0039M-14
- Banik, D., He, R., Lu, N., & Feng, Y. (2024). Mitigation mechanisms of alkali silica reaction through the incorporation of colloidal nanoSiO₂ in accelerated mortar bar testing. *Construction and Building Materials*, 422, 135834. <https://doi.org/10.1016/j.conbuildmat.2024.135834>
- Barrett, T. J. (2013). *Performance of portland limestone cements: Cements designed to be more sustainable that include up to 15% limestone addition* [Master's thesis, Purdue University]. Purdue e-Pubs. <https://docs.lib.purdue.edu/dissertations/AAI1549298/>
- Barrett, T. J., Sun, H., Nantung, T., & Weiss, W. J. (2014). Performance of portland limestone cements. *Transportation Research Record*, 2441(1), 112–120. <https://doi.org/10.3141/2441-15>
- Bu, Y., Spragg, R., & Weiss, W. J. (2014). Comparison of the pore volume in concrete as determined using ASTM C642 and vacuum saturation. *Advances in Civil Engineering Materials*, 3(1), 308–315. <https://doi.org/10.1520/ACEM20130090>
- Diamond, S., & Huang, J. (2001). The ITZ in concrete—a different view based on image analysis and SEM observations. *Cement and Concrete Composites*, 23(2–3), 179–188. [https://doi.org/10.1016/S0958-9465\(00\)00065-2](https://doi.org/10.1016/S0958-9465(00)00065-2)
- Gao, Y., De Schutter, G., Ye, G., Huang, H., Tan, Z., & Wu, K. (2013). Porosity characterization of ITZ in cementitious composites: Concentric expansion and overflow criterion. *Construction and Building Materials*, 38, 1051–1057. <https://doi.org/10.1016/j.conbuildmat.2012.09.047>
- Gao, Y., De Schutter, G., Ye, G., Tan, Z., & Wu, K. (2014). The ITZ microstructure, thickness and porosity in blended cementitious composite: Effects of curing age, water to binder ratio and aggregate content. *Composites Part B: Engineering*, 60, 1–13. <https://doi.org/10.1016/j.compositesb.2013.12.021>
- He, R., Nantung, T., Olek, J., & Lu, N. (2023). Field study of the dielectric constant of concrete: A parameter less sensitive to environmental variations than electrical resistivity. *Journal of Building Engineering*, 74, 106938. <https://doi.org/10.1016/j.job.2023.106938>
- Lothenbach, B., Le Saout, G., Gallucci, E., & Scrivener, K. (2008). Influence of limestone on the hydration of portland cements. *Cement and Concrete Research*, 38(6), 848–860. <https://doi.org/10.1016/j.cemconres.2008.01.002>

- Lyu, K., She, W., Miao, C., Chang, H., & Gu, Y. (2019). Quantitative characterization of pore morphology in hardened cement paste via SEM-BSE image analysis. *Construction and Building Materials*, 202, 589–602. <https://doi.org/10.1016/j.conbuildmat.2019.01.055>
- McZgee, V. E., & Carleton, W. T. (1970). Piecewise regression. *Journal of the American Statistical Association*, 65(331), 1109–1124. <https://doi.org/10.1080/01621459.1970.10481147>
- Nadelman, E. I., & Kurtis, K. E. (2019). Durability of portland-limestone cement-based materials to physical salt attack. *Cement and Concrete Research*, 125, 105859. <https://doi.org/10.1016/j.cemconres.2019.105859>
- Odler, I. (1998). Hydration, setting and hardening of Portland cement. In P. C. Hewlett (Eds.), *Lea's Chemistry of Cement and Concrete* (4th ed., pp. 241–297). <https://doi.org/10.1016/B978-075066256-7/50018-7>
- Ollivier, J. P., Maso, J. C., & Bourdette, B. (1995). Interfacial transition zone in concrete. *Advanced Cement Based Materials*, 2(1), 30–38. [https://doi.org/10.1016/1065-7355\(95\)90037-3](https://doi.org/10.1016/1065-7355(95)90037-3)
- Quennoz, A., & Scrivener, K. L. (2012). Hydration of C₃A-gypsum systems. *Cement and Concrete Research*, 42(7), 1032–1041. <https://doi.org/10.1016/j.cemconres.2012.04.005>
- Scrivener, K. L., Crumbie, A. K., & Laugesen, P. (2004). The interfacial transition zone (ITZ) between cement paste and aggregate in concrete. *Interface Science*, 12, 411–421. <https://doi.org/10.1023/B:INTS.0000042339.92990.4c>
- Sersale, R., Cioffi, R., Frigione, G., & Zenone, F. (1991). Relationship between gypsum content, porosity and strength in cement. I. Effect of SO₃ on the physical microstructure of portland cement mortars. *Cement and Concrete Research*, 21(1), 120–126. [https://doi.org/10.1016/0008-8846\(91\)90038-J](https://doi.org/10.1016/0008-8846(91)90038-J)
- Tennis, P. D., Thomas, M. D. A., & Weiss, W. J. (2011). *State-of-the-art report on use of limestone in cements at levels of up to 15%* (SN3148) Portland Cement Association. https://www.fcpa.org/wp-content/uploads/Use_of_Limestone_in_Cements_up_to_15_percent.pdf
- Tsilivilis, S., Tsantilas, J., Kakali, G., Chaniotakis, E., & Sakellariou, A. (2003). The permeability of portland limestone cement concrete. *Cement and Concrete Research*, 33(9), 1465–1471. [https://doi.org/10.1016/S0008-8846\(03\)00092-9](https://doi.org/10.1016/S0008-8846(03)00092-9)
- United States Environmental Protection Agency. (2021, October). *U.S. cement industry carbon intensities (2019)*. <https://www.epa.gov/system/files/documents/2021-10/cement-carbon-intensities-fact-sheet.pdf>
- Vuk, T., Tinta, V., Gabrovšek, R., & Kaučič, V. (2001). The effects of limestone addition, clinker type and fineness on properties of Portland cement. *Cement and Concrete Research*, 31(1), 135–139. [https://doi.org/10.1016/S0008-8846\(00\)00427-0](https://doi.org/10.1016/S0008-8846(00)00427-0)
- Wang, B., Yan, L., Fu, Q., & Kasal, B. (2021). A comprehensive review on recycled aggregate and recycled aggregate concrete. *Resources, Conservation and Recycling*, 171, 105565. <https://doi.org/10.1016/j.resconrec.2021.105565>
- Wang, D., Shi, C., Farzadnia, N., Shi, Z., Jia, H., & Ou, Z. (2018). A review on use of limestone powder in cement-based materials: Mechanism, hydration and microstructures. *Construction and Building Materials*, 181, 659–672. <https://doi.org/10.1016/j.conbuildmat.2018.06.075>
- Wang, Y., Zhang, W., Wang, J., Huang, R., Lou, G., & Luo, S. (2024). Effects of coarse aggregate size on thickness and micro-properties of ITZ and the mechanical properties of concrete. *Cement and Concrete Composites*, 154, 105777. <https://doi.org/10.1016/j.cemconcomp.2024.105777>
- Wong, H. S., & Buenfeld, N. R. (2006). Euclidean distance mapping for computing microstructural gradients at interfaces in composite materials. *Cement and Concrete Research*, 36(6), 1091–1097. <https://doi.org/10.1016/j.cemconres.2005.10.003>
- Wong, H. S., Head, M. K., & Buenfeld, N. R. (2006). Pore segmentation of cement-based materials from backscattered electron images. *Cement and Concrete Research*, 36(6), 1083–1090. <https://doi.org/10.1016/j.cemconres.2005.10.006>
- Wu, K., Shi, H., Xu, L., Ye, G., & De Schutter, G. (2016). Microstructural characterization of ITZ in blended cement concretes and its relation to transport properties. *Cement and Concrete Research*, 79, 243–256. <https://doi.org/10.1016/j.cemconres.2015.09.018>
- Xu, G., & Beaudoin, J. J. (2000). Effect of polycarboxylate superplasticizer on contribution of interfacial transition zone to electrical conductivity of Portland cement mortars. *ACI Materials Journal*, 97(4), 418–424.

About the Joint Transportation Research Program (JTRP)

On March 11, 1937, the Indiana Legislature passed an act which authorized the Indiana State Highway Commission to cooperate with and assist Purdue University in developing the best methods of improving and maintaining the highways of the state and the respective counties thereof. That collaborative effort was called the Joint Highway Research Project (JHRP). In 1997 the collaborative venture was renamed as the Joint Transportation Research Program (JTRP) to reflect the state and national efforts to integrate the management and operation of various transportation modes.

The first studies of JHRP were concerned with Test Road No. 1 — evaluation of the weathering characteristics of stabilized materials. After World War II, the JHRP program grew substantially and was regularly producing technical reports. Over 1,600 technical reports are now available, published as part of the JHRP and subsequently JTRP collaborative venture between Purdue University and what is now the Indiana Department of Transportation.

Free online access to all reports is provided through a unique collaboration between JTRP and Purdue Libraries. These are available at docs.lib.purdue.edu/jtrp/.

Further information about JTRP and its current research program is available at engineering.purdue.edu/JTRP.

About This Report

An open access version of this publication is available online. See the URL in the citation below.

Sung, J., He, R., Lu, N., & Feng, Y. (2025). *Systematic study of type 1L cement for mixture optimization and carbon reduction* (Joint Transportation Research Program Publication No. FHWA/IN/JTRP-2025/27). West Lafayette, IN: Purdue University. <https://doi.org/10.5703/1288284318575>